PNAS

Supporting Information for
High-Throughput Experimentation for Discovery of Biodegradable Polyesters.

Katharina Fransen*, Sarah H. M. Av-Ron*, Tess R. Buchanan, Dylan J. Walsh, Dechen T. Rota, Lana Van Note, Bradley D. Olsen[†]
Department of Chemical Engineering, Massachusetts Institute of Technology, Cambridge MA 02139
*equal contributions

[†]Corresponding author: Bradley D. Olsen
Email: bdolsen@mit.edu

This PDF file includes:

Other supporting materials for this manuscript include the following:

I. Table of Contents

II. Polymer Library Design

a. Library Design Constraints

In addition to design parameters for monomer selection, the polymer library also had constraints that affected the scope of the project. Petroleum and sustainably based monomers were both used in order to maximize the number of monomers which could be purchased in quantities relevant for high throughput synthesis at a price of less than $100 per gram. This was to ensure that there was enough material for a reasonable number of functional group representations to be able to draw generalized conclusions about the impact of certain chemical functionalities while staying within reasonable materials costs. Additionally, only monomers containing functional groups using oxygen, nitrogen, and sulfur heteroatoms were considered since these were considered the most relevant to polyester and polycarbonate materials with potential commercial relevance and scalable bio-sourcing.

Materials. All materials were purchased commercially from Sigma Aldrich, TCI America, Alfa Aesar, Enamine, or Fisher Scientific. With the exception of β-propiolactone, δ-valerolactone, ε-caprolactone, undecanoic δ-lactone, δ-nonalactone, and 5-dodecanolide, all reagents were used as received. β-propiolactone, δ-valerolactone, ε-caprolactone, undecanoic δ-lactone, δ-nonalactone, and 5-dodecanolide were dried over calcium hydride and distilled under vacuum before use.

Monomer Information. Information on the monomers included in the library is provided in *Table S1*. Monomer names and SMILES descriptors are included, in addition to the number of polymers in which each monomer is used in the library, as well as which chemical functionalities it provides. A few monomers were purchased for the library synthesis and were unable to be successfully polymerized. The name, chemical structure, SMILES descriptor, and explanation for failure is provided in *Table S2.*

Polymers in the Library. The polymer library is comprised of 660 polymers, of which 642 have unique chemical structures. Duplicate polymers were synthesized through different synthetic approaches for monomers with double and triple bonds as well as some ethers, with the acid chloride synthesis being preferentially used for the biodegradation data set due to the potential for cross-linking and degradation from conditions used during melt polymerizations. The successfully synthesized polymers, along with a general synthesis type are summarized in *Figure S1.* The details of the successful polymers in the library, including M_w, M_n, dispersity, ratio of monomers (if relevant), and a BigSMILES(1) descriptor are provided in *Supplementary Dataset S4.* Additionally, a reaction procedure key for the synthetic procedure used is provided. The reaction procedures and keys are detailed in *Table S3*.

b. Synthesis Procedures

Reaction type and reaction conditions were selected based on the monomers used in each reaction. Diol monomers were all tested for reaction with acid chlorides; however, only those which were not aromatic were used for melt polycondensation reactions. Diols with double and triple bonds were reacted under melt polycondensation conditions; however, it should be noted that these polymers are potentially branched and many were also synthesized using acid chloride interfacial reaction conditions for further data analysis. Solution ring opening polymerizations were performed with monomers such as lactide and ε-caprolactone which have been shown to react under such conditions.(2, 3) However, it was found that many ring opening monomers were only or more compatible with melt conditions, and reactions were performed as such. It was additionally noted that the concentrations of Tin (II) octoate used in synthesis with a subset of ring opening polymerizations inhibited bacterial growth necessary for biodegradation testing. These polymers were additionally purified. While polymers were characterized using GPC and NMR when possible, a large number of samples were not soluble in available GPC or NMR solvents. Polymerization reaction products were screened for polymer products through the preparation of sample plates for the biodegradation clear zone assay. Monomers were DCM soluble, so products insoluble in DCM were considered polymeric. Additionally, the opacity of the plate was evaluated, with clear plates suggesting that polymerization had not occurred, the polymer was water soluble, or the polymer was too close in refractive index to the agar gel. In addition to characterizations described in the main manuscript, polymerization reaction products were screened for polymer products through the preparation of sample

plates for the biodegradation clear zone assay. Monomers were DCM soluble, so products insoluble in DCM were considered polymeric. Additionally, the opacity of the plate was evaluated, with clear plates suggesting that polymerization had not occurred, the polymer was water soluble, or the polymer was too close in refractive index to the agar gel. Only three polymers for which GPC indicated high molecular weight were observed to not show opacity on clear zone plates. These polymers are included in the last three rows of *Supplementary Dataset S4* as part of the synthesized library, but are noted as not being included in the biodegradation dataset using a '*' by their number in the polymer library.

c. Melt Polycondensation Reactions

Three subsets of melt condensation reactions were performed. The first was between dicarboxylic acids and diols, the second between all diols (including aromatics not otherwise used in melt reactions) and dimethyl carbonate to obtain polycarbonates, and the third was between different ratios of hydroxyacids. Reactions were run in batches of 11 reactions using either a ChemGlass OPTIBLOCK parallel synthesis reaction block system with a customized machined gas/vacuum splitter (*Supplementary Information Figure S3*) or a ChemGlass Reaction Block for circular top hot plate stirrers and a tubing-based gas/vacuum adapter. These systems are pictured in *Figure* S2. The reaction conditions for each batch, specifically the temperature, pressure, and time of each condition, were tuned based on the monomers in the synthetic batch. The minimum synthesis temperature was selected as the lowest diol melting temperature for diols in the batch of polymers. As the reaction proceeded and changes in viscosity were observed, indicating the formation of oligomers, the temperature of the reactions was increased in stages. After between 4 and 6 hours of reaction, vacuum (~10 mmHg or ~25mmHg) was applied overnight. Details of the reaction conditions used for each batch are found in *Table S3*. Specific masses and volumes of reagents used in each synthesis are provided in *Dataset S1* for successful reactions and *Dataset S2* for unsuccessful reactions. For reactions with two different hydroxy-acids, the final monomer ratio was determined via H^1 NMR.

For several monomer combinations, melt conditions could not be achieved. Of particular note, 2,6-naphthalenedicarboxylic acid, [(carboxymethyl)(methyl)amino]acetic acid, and 2,5-furandicarboxylic acid were not able to melt under any tested reaction conditions. As a result, 2,5-furandicarboxylic acid was replaced with 2,5-furandicarboxylic acid methyl ester for all polymerizations. 2,6-naphthalenedicarboxylic acid and [(carboxymethyl)(methyl)amino]acetic acid were successfully reacted with diols which could, when melted, solubilize the two dicarboxylic acids. In particular, these were generally diols which had comparable or larger molecular weight than the dicarboxylic acid being used. Monomer combinations which did not yield polymers and their reaction conditions are detailed in *Table S4*. Specific masses and volumes of reagents used in each synthesis are provided in *Dataset S1* for successful reactions and *Dataset S2* for unsuccessful reactions.

d. Acid Chloride Condensation Reactions

Two different approaches yielded condensation polymers using diols and acid chloride monomers. The first was a solution approach with stoichiometric pyridine. The second was an interfacial polymerization approach with base added to the diol solvent to quench developed chloride ions. The interfacial acid chloride polymerization reactions had a 53% success rate, with a drop in success rate due to side reactions between the acid chlorides and water as well as solubility limitations of the growing polymer chains in the chosen solvents. The monomer combinations which did not yield polymers for these reactions are tabulated in *Table S4*. The solvent system most compatible with the monomers used was selected; however, exploration of solvent systems was not exhaustive.(4, 5) The solution and interfacial procedures are found in *Table S3*. Information on the specific monomer masses, solvents, and base used in each reaction are provided in *Dataset S1* for successful reactions and *Dataset S2* for unsuccessful reactions..

e. Ring Opening Polymerization

Ring-opening polymerizations were used for lactone-ring monomers, including glycolide and lactide. Previously shown solution polymerization methods(3) were applied to lactide, glycolide, δ-valerolactone, ε-caprolactone, and β-propiolactone. Glycolide-containing polymers produced via solution methods were reproduced via a melt approach, and polymers included in the polymer table reference those produced via melt reactions, as indicated by the method key listed in *Supplementary Table S3*. All other

reactions were run in a melt with triphenyl bismuth and tin (II) octoate as catalysts.(6) In order to increase the number of polymers which contained these monomers in the library, pairs of monomers were reacted with each other in 2 to 1 and 1 to 2 molar ratios as material supplies allowed. The ratio of monomers in the polymer product was determined by NMR when dissolution of the polymer in appropriate solvents was possible and can be found in *Table S3*. Polymers for which the monomer ratio could not be resolved due to overlapping peaks are noted as 'NR'. Reactions which used tin (II) octoate were purified over aluminum oxide to remove the tin before being precipitated and dried for biodegradation testing. Procedures used for all reactions are summarized in *Table S3,* polymers are included in *Supplementary Table S3,* and additional tested reaction combinations are included in *Table S4*. Details of the reactions are found in *Dataset S1* for successful reactions and *Dataset S2* for unsuccessful reactions..

III. High-throughput clear zone biodegradation testing

a. Microorganism selection

Multiple criteria are required of the selected strain for the clear zone biodegradation testing. The strain must be proven to degrade positive control polymers. In this study poly(hydroxy-3-buterate) (P3HB) was used as the positive control. Second, the strain should be found in natural environments of relevance for the test, and not be highly specific to a single location. *Pseudomonas lemoignei* (*P. lemoignei*) also called *Paucimonas lemoignei*, has been identified across multiple studies as a PHA degrading strain.(7-9) At least five PHA depolymerase genes have been identified,(10) generating at minimum two types of extracellular enzymes able to degrade short chain length PHA (PHAscl) of either native or denatured PHA granules.(11) This makes *P. lemoignei* to more likely be able to degrade a wide range of PHAs, with ranging levels of crystallinity.

b. Growth medium

The recipe was made following the ATCC 179 *Pseudomonas* growth medium, composed of basal medium, solution A and solution B. Double concentrated basal medium was prepared by adding 2.56 g K_2HPO_4, 2.08 g KH_2PO_4, 1.0 g NH_4Cl and 0.247 g anhydrous $MgSO_4$ in 500 mL MilliQ water. The solution's pH was adjusted to 6.8 using NaOH and then filter-sterilized. Solution A was prepared by adding 1.0 g of ferric ammonium citrate and 0.1 g $CaCl_2$ to 100 mL MilliQ water and then filter-sterilized. Solution B is a 1.0 M succinic acid solution adjusted to pH 6 with NaOH and filter sterilized. The microorganism growth medium is composed of 50 µL of solution A and 150 µL of solution B for 5 mL of double concentrated basal medium.

c. Sample preparation and selection

Figure S4 illustrates the sample preparation process with inoculation and incubation. For each tested polymer, 40 mg was weighed and added to a 5.54 mL vial (1.5 dram). 0.8 mL of dichloromethane (DCM) was added, and the vial was left on a plate shaker for mixing for at least 30 min prior to plate making. 16 mL of double concentrated basal medium was added to an 80 mL conical vial and kept in a 60 °C water bath. 20 mL of autoclave sterilized 40 g/L agars was added to the conical vial. 4 mL of double concentrated basal medium was added to the polymer vial which was then vigorously shaken by hand for about 5 sec, after which the vial content appeared milky due to the emulsification of the DCM in the aqueous phase. The content of the polymer vial was immediately poured into the conical vial still in the water bath at 60 °C. The DCM was left to bubble off for 30 sec during which the homogenizer probe was placed in the vial. Then the homogenizer was turned on at 10,000 rpm for 15 sec, turned off for 15 sec, and turned on one more time for 15 sec. The vial was then promptly brought to a sterilized benchtop, and all subsequent procedures were performed using sterile technique. 10 mL of the solution was added to a 15 mL conical tube containing 50 µL of solution A and 150 µL of solution B. The conical tube was turned upside down gently 3 times to mix the content without generating bubbles. 0.8 mL of the solution from the conical tube was added with a sterile pipette to wells A1, A2, A3, A4, B1, B4, C1 and C4 as shown in *Figure S5*. The final polymer concentration was 1 g/L in growth medium agar, as previously used in clear zone assays.(12, 13) Wells B2, B3, C2 and C3 were filled with 0.8 mL of no-polymer control made of equal volumes of double concentrated growth medium and 40 g/L concentrated agar.

In some cases, sample wells containing polymer would appear as clear as the control wells. In some cases, the clearness was due to a low molecular weight (MW) and a second synthesis attempt was made to increase the polymer MW. For any other sample, the polymers could not be tested for biodegradability using the clear zone method and were thus marked as untestable. Such unsuccessful samples are marked in *Figure S1*.

d. Microorganism conservation and growth for inoculation

P. lemoignei was conserved as freezer stock in growth medium with added sterile glycerol at a 30% volume content. For clear zone sample inoculation, 2 mL of double concentrated growth medium and 2 mL of sterile milli-Q water were added to a test tube. The freezer stock was stabbed five times with a sterile pipette which was then dropped in the test tube. The test tube was left in an incubating shaker for about 40 hours at 30 °C and 180 rpm. The inoculation solution had a final OD between 0.5 and 0.8.

e. Inoculation and clear zone testing

The polymer samples were then inoculated with 1 µL of the *P. lemoignei* inoculation solution. Each polymer-agar mixture had its own surface properties, and some led to a high initial spread of the cell solution while inoculating. To ensure statistical validity of the results, each sample was replicated such that there were at least 3 replicates with colonies smaller than 6 mm in width along the largest axis. Plates were then placed with lids on in an incubator at 30 °C with a water source to prevent the agar from drying.

Biodegradation monitoring was performed by taking well pictures with backlighting to measure the light able to go through the sample wells. The system for clear zone monitoring was an Opentrons OT-1 1st generation robot with a 2.8-12mm Varifocal Usb Webcam Mini Camera with adjustable focus fixed to the mobile pipettor arm. The 12-well plate was placed on a fixed holder to have wells at identical positions at each measurement. An 8x11 inch Kaiser Slimlite Plano tablet was used for backlighting; it was placed underneath the plate holder and kept at constant lighting intensity. A blackout cutout of the wells was placed under the well plate holder to only have backlighting right under the wells. *Figure S6* shows pictures of the setup. A python script (provided on GITHUB) was written to perform the 12 pictures of each 12-well plate measurement, with each picture being centered on a well.

The time zero measurement for the clear zone biodegradation test was done within 2 hours after inoculation. Biodegradation monitoring was done every 8 hours for the first 6 days on incubation, then on the 7th, 9th, 11th and 13th days. Each measurement was labeled with a time stamp in minutes for precise data analysis. The incubator water source led to water condensation on the well plate lids. Therefore, before each measurement, the lids were wiped with a paper towel and passed over a Bunsen burner to sterilize.

Some polymers prevented bacterial growth due to the toxicity of the monomer or the catalyst. Those samples were still tested for biodegradation as hydrolysis could still occur. *Table S6* lists all the samples that did not have bacterial growth.

f. Particle size estimation

To determine the average particle size in the biodegradation samples, agar polymer solutions were prepared as described above, and about 5 mL of solution was pipetted onto one side of a vertical microscope slide. The solution was allowed to flow off the slide, leaving behind a thin film of hardened agar. The slide was then observed under the microscope to optically image particle sizes. Three different samples were observed: a DCM soluble polymer that had a classic clear zone degradation behavior, the P3HB control non-soluble in DCM but displaying a classic clear zone behavior, and a non-soluble polymer that was determined not biodegradable by the strain. The images were analyzed with a custom Python code using a kmean color quantization code on Python (available on Zenodo),(14) with a cluster size of 2. This allowed automatic particle detection in the image according to shading. Results and particle size distributions are shown in *Figure S15*.

g. Physical state and dichloromethane solubility evaluation

To determine the physical state of each polymer, all the polymer vials were placed on their side and left for 3 days. Any polymer that flowed to the side of the vial was marked as viscous (i.e. above any glass transition or melting temperature). For all the other samples marked as solid, crystallinity was

determined by imaging under polarized optical microscopy. A small amount of polymer (between 1 mg to 20 mg) was dissolved in dichloromethane at a concentration of 40 mg/mL. The solution was left on a plate shaker for at least 30 min, with additional vigorous manual shaking before and after. Samples that had visible particles left in the solution were marked as insoluble in dichloromethane. The solubility classification of each polymer is shown in *Figure S14*, and the distribution of this classification and its relationship to biodegradation is shown in *Figure S13*. A small drop of the solution was then deposited on a microscope slide and left to dry. The thin film was observed by polarized optical microscopy with a x20 magnification. If any crystal was observed in the sample, the polymer was marked as crystalline. Otherwise, it was marked as amorphous. The individual physical state classification of each polymer is shown in *Figure S12*, and the distribution of this classification and its relationship to biodegradation is shown in *Figure S11*. Tabulated information on the solubility in dichloromethane and physical state of the polymers is found in *Dataset S3*.

h. Data analysis and biodegradability determination

Images were analyzed using a semi-automated process to extract transmission curves. The main steps are image processing and center determination, defect masking, shading curve generation and degradation categorization, time measurement cleanout, degradation determination and degradation time estimation. All steps are accomplished in Python with the OpenCV, scipy and matplotlib libraries.

Image processing and center determination (Figure S17 and S18): Pictures are changed into B/W scale and cropped into a tight square around the center well. The next step is to locate the colony in the center of the well. The list measurement image is used to determine the center for the full series of measurement of a given well, a median filter of kernel size 7 is applied to the image 10 times to increase contrast between the darker colony and the rest of the agar plate, and a mask is applied to the image to hide the well plate around the agar. The resulting image is then displayed, and the user must click on the colony, aiming for darker colored pixels. The color of the clicked pixel is then used to filter the image and select all connected pixels that are similarly dark or darker. The resulting detected colony is then displayed to the user to verify that the process worked properly. The center of mass of the detected colony is then set as the center and the size of the colony is computed from the largest distance between two pixels of the colony. If there is no colony, the user can select the top left button "No colony". The center is set as the center of the image and the size of the colony is set to zero.

Defect masking (Figure S19): For this step, the last measurement cropped image of a given well with no additional processing is displayed to the user. If there are any visible scratches on the image (from scratches on the lid of the well plate), the user must successively click around the defect, clockwise or counterclockwise until the defect is tightly contained around the appearing clicks. Once finished, the user selects "End" in the top left corner. If there are no defects, the user clicks on "none" in the bottom left corner.

Shading curve generation and time measurement cleanout (Figure S20-S22): For each well and time measurement, a shading curve is generated. Starting from the detected center in the first step, the shading curve has the value of the average color of a donut of 3-pixel thickness and of given radius. To have proper overlap of the curves, the two uninoculated controls containing no polymer (wells B2 and B3) were used to determine the y-axis displacement that each time measurement needed to overlap perfectly with the time zero curve; these controls should not be changing throughout the time of the incubation. The shading curves are then transformed into normalized OD curves by first adding the computed displacement, and then subtracting the time zero curve to all other shading curves for a given well before applying the log. To account for measurement errors such as improper placement of the plate in the holder or improper blackout of the measurement robot, the user is asked to delete time-specific shading curves when they fail to properly overlap with the other time measurements. For each well, a plot is displayed with all the time measurement OD curves, and the user needs to click on a defective curve to delete it. The plot is displayed again without the previously clicked curves. When all the displayed curves are satisfactory, the user presses below the "Done" button on the bottom left.

Degradation determination (Figure S23 and S24): The integration of each OD curve between distance to center of 3.7 and 7.0 is computed, and all the replicates' integration values are plotted according to measurement time. The user needs to click to indicate the time points to include in the degradation "rate"

calculation, finding the linear trend, or selecting all the data if there is no trend. The sample will be determined as biodegradable if the average slope of the replicates is more than that of the no polymer inoculated controls (wells C2 and C3), with a difference of at least 1 standard deviation. If the average slope changes signs when 1.5 standard deviation is added or subtracted, the sample is marked as non-degradable. For samples marked as degradable, the user is asked to select the degradation behavior of the sample. A plot with all the OD curves of a well plate is displayed, and the user selects the button corresponding to the degradation behavior. Degradability classification is included in *Dataset S3*.

Degradation time estimation (*Figure S25)*: For each well of a degrading sample, the cleaned-out OD curves are displayed for a distance to center ranging from 3.7 to 7.0mm (corresponding to next step integration region). The user needs to click on the curve that shows first signs of degradation and then the last curve showing signs that degradation is still progressing. If the starting and ending curves are hard to find due to the tightness of the curves and changes, the user can click on the bottom left under the word "Done" to automatically select the first or last measurement times. With a starting and end time for each well, the degradation time may be computed, and then average this value over all the valid replicates. The results are shown in *Figure S*16.

IV. Biodegradation classification and prediction

a. Vectorization

The first step to develop machine-learning models was to vectorize each polymer. Established fingerprinting methods for small molecules were used to represent chemical structures. To generate a deterministic structure representing the ensemble of polymer molecules that could be used for fingerprinting, a strategy applied by A. Arora(15) was employed: each AB polymer is written as an 8-repeat ring oligomer with the first and last atoms joined together, with A and B head-to-head and head-to-tail alternation if monomers were non-symmetric. This method effectively approximates the polymer as infinite molar mass as the fingerprint does not change as more monomers are incorporated into the ring. For polymers with monomer ratios of 2:1, the repeat unit was AAB. Examples of such SMILES rings are shown in *Table S8*.

Each SMILES ring was vectorized using the sci-kit learn python library,(16) generating Morgan fingerprints, RDKit fingerprints and RDKit descriptors. The list of RDKit descriptors used is listed in *Table S7*. Fingerprint vector sizes were optimized, and the range of generated vector sizes was 50 to 600 by increments of 50. After fingerprints were generated, any vector feature that was identical for all polymers of the dataset was eliminated, which led to slightly smaller vector sizes used in the actual fits. The final vector sizes studied for optimization are listed in *Table S10*.

Polymers that were DCM soluble during the crystallinity determination study and all viscous polymers have their physical state properly determined, and this can be used as an input vector for the machine learning modeling. Physical state was encoded as a one hot vector to indicate fluid, glassy or crystalline, adding three features to the chemical description vector. Polymers that could have molecular weight determined by GPC measurement form another subset with three additional features: Mw, Mn and dispersity. Finally, a subset of polymers with both physical state and GPC data was formed, where the full set of features had six additional columns compared to just chemical description. Each feature for each dataset or subset was restricted to reach values between -1 and 1 by dividing the feature column by the maximum occurring value for this feature. No further normalization was performed.

b. Data splits for training, testing and validation

The dataset has many different chemistries, with some of them represented by only a few members. This makes data splitting tricky, as model performance is more accurately evaluated when each split contains similar information. Therefore, to make the splits, the data was first separated by biodegradability. The degrading and non-degrading parts were then split into 6 equal parts randomly. To recombine the now 12 parts of the dataset, each of the 6 splits were ordered according to the number of polymers containing nitrogen (as it is one of the rarer features in the dataset, but of great interest). The split with the fewest nitrogen-containing-polymers from the degrading half was combined with the split with the most nitrogen-containing-polymers from the non-degrading half. The same logic was applied to the second

fewest and most nitrogen-containing-polymers splits of the degrading and non-degrading half, respectively. So on until all splits are combined, and the result is the full dataset split in 6 equal parts with 50% degrading polymers and approximately the same number of nitrogen-containing-polymers.

To ensure the proper distribution of special chemistries in each split, the fraction of each of these chemistries was plotted (see *Figure S26*). If the distribution of any chemistry was out of balance, the random seed selected for the initial 6-way-splits of the degrading and non-degrading parts was changed, and the full process was repeated. This process is illustrated in *Figure S27*. The data of each confusion matrix is shown in *Table S12*.

c. Hyperparameter optimization

Machine learning models were studies using the sci-kit learn python library. For random forest modeling, the hyperparameters that were adjusted were the total number of trees, the maximum depth for each tree, the maximum number of leaves per tree, and the chemical description fingerprinting vector size. Minimum sample to split and minimum number of samples per node was set to 2 and 1 respectively for all models. All combinations of parameter values were tested, and optimal hyperparameter values were found by averaging all the accuracies of any run with the studied hyperparameter set to the value of interest. The results of these averages are shown in *Figures S28* to *S31*. The optimal hyperparameters for random forest models are summarized in *Table S11*. For logistic classification modeling, vector size was optimized by selecting the value that led to the highest testing accuracy (see *Figure S32 and S33*). The testing accuracy for the optimal hyperparameters is shown in the main manuscript *Figure 5*.

d. Datasets chemical diversity study

The chemical diversity of each dataset was established using the Tanimoto scoring(17). Using the Python RDKit library, a 2048 sized RDKit fingerprint was generated for each chemistry using the polymers' 8 repeat rings SMILE strings described above. Each polymer pair was used as input in the TanimotoSimilarity function from the RDKit library, and the values for each dataset were plotted as a histogram as shown in *Figure S35*. The plots show the average and the standard deviation of the distribution of scores for each dataset.

e. Machine learning negative control

For the data subset using molecular weight and physical state data, a negative control run was done using the features for this information without any chemical descriptors. The optimization results for the random forest model is shown in *Figure S37*. The testing and validation accuracy for this subdataset is shown in *Figure S38*.
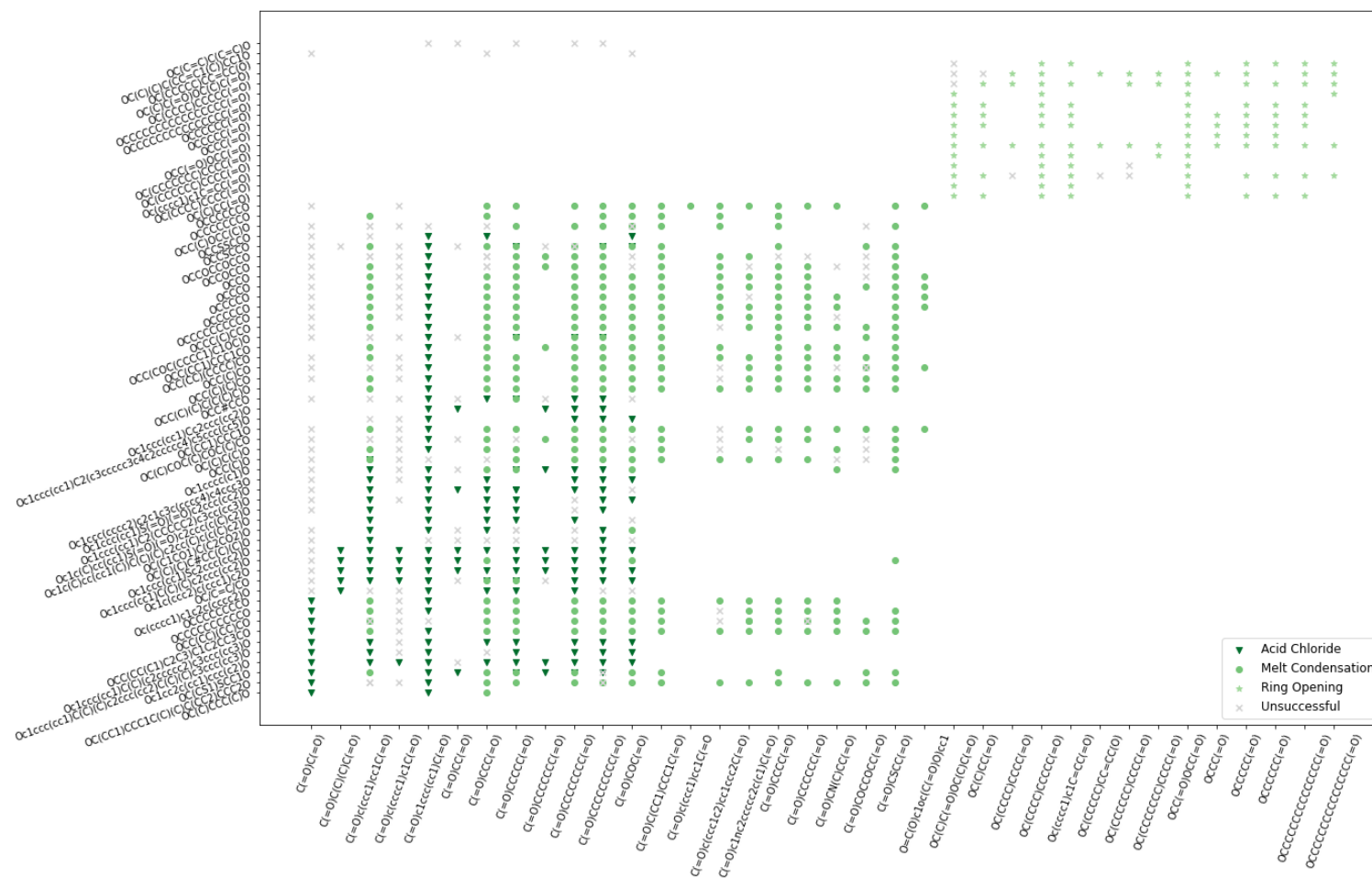
V. Figures

Figure S1: Overview of library synthesis efforts and containing monomer composition. The SMILES of repeat unit structures of the monomers are plotted on the axes. Carboxylic acids (or their acid chloride counterpart) are plotted on the x-axis in addition to lactone ring monomers. Diols are plotted on the y-axis, with the hydroxy-acid monomers and lactone rings being repeated. Each point represents a combination of monomers tested. Unsuccessful reactions are shown in gray.
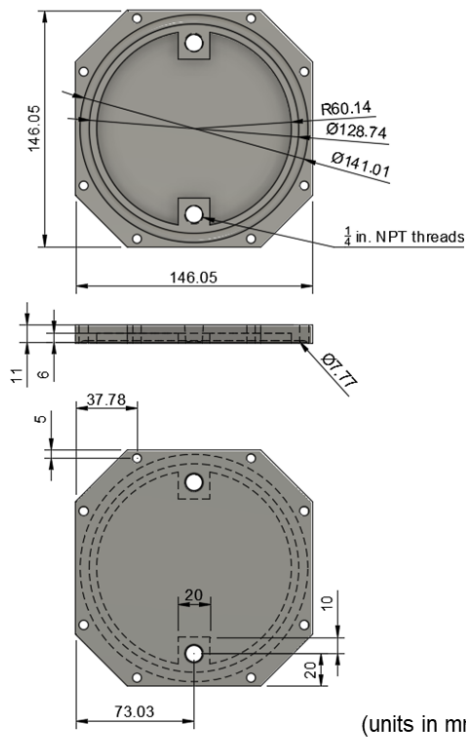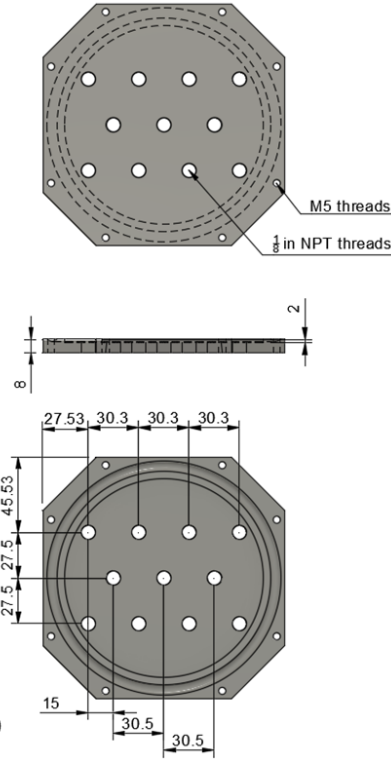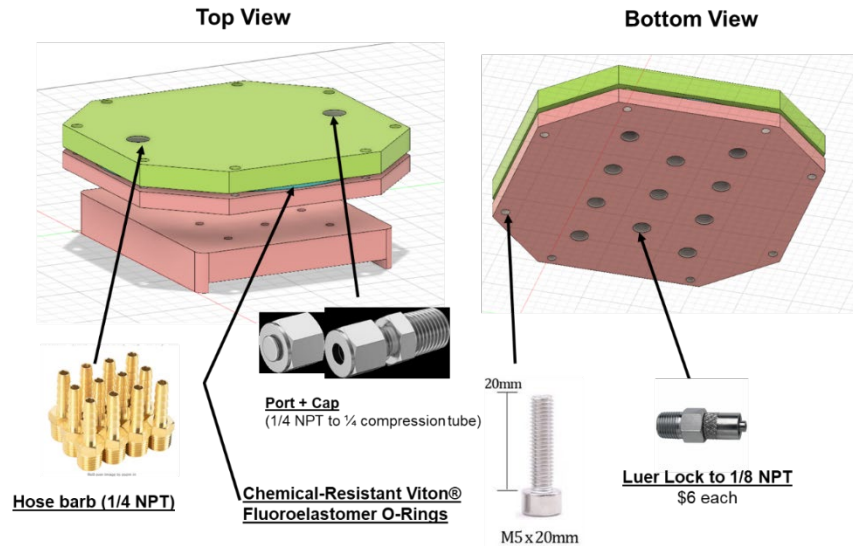
A

B

(units in mm)

C

Top View   Bottom View

Port + Cap
(1/4 NPT to 1/4 compression tube)

20mm

Hose barb (1/4 NPT)

Chemical-Resistant Viton®
Fluoroelastomer O-Rings

M5 x 20mm

Luer Lock to 1/8 NPT
$6 each

Figure S2: Custom vacuum block splitter. **A:** Technical drawings for air manifold. Left: Top part of air manifold. Right: Bottom part of air manifold. **B:** Photographs of manufactured parts of the air manifold. **C:** Diagram of the assembly of the air manifold and assorted parts. Hose barbs (Brass Barbed Hose Fitting for Air and Water, Straight Adapter for 1/4" Hose ID, 1/4 NPTF Male), the o-ring (Chemical-Rst Viton® Fluoroelastomer O-Ring 1/8 Fractional Width, Dash Number 251), port (Yor-Lok Fitting for Stainless Steel Tubing Straight Adapter for 1/4" Tube OD X 1/4 NPT Male) and cap (Cap for 1/4" Tube OD Yor-Lok Fitting), and luer lock to NPT adapters (Brass Quick-Turn Tube Coupling for Air Plug, 1/8 NPT Male) were purchased from McMaster Carr. M5 bolts were purchased from Amazon.
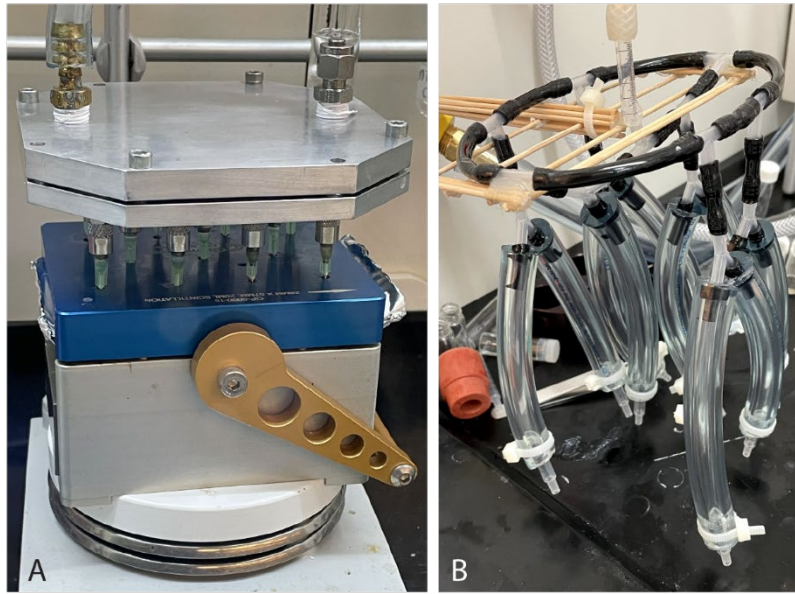
Figure S3: Melt synthesis equipment. A: OPTIBLOCK Synthesis block with custom vacuum splitter. B: Tubing-based vacuum splitter for use with individual vials.
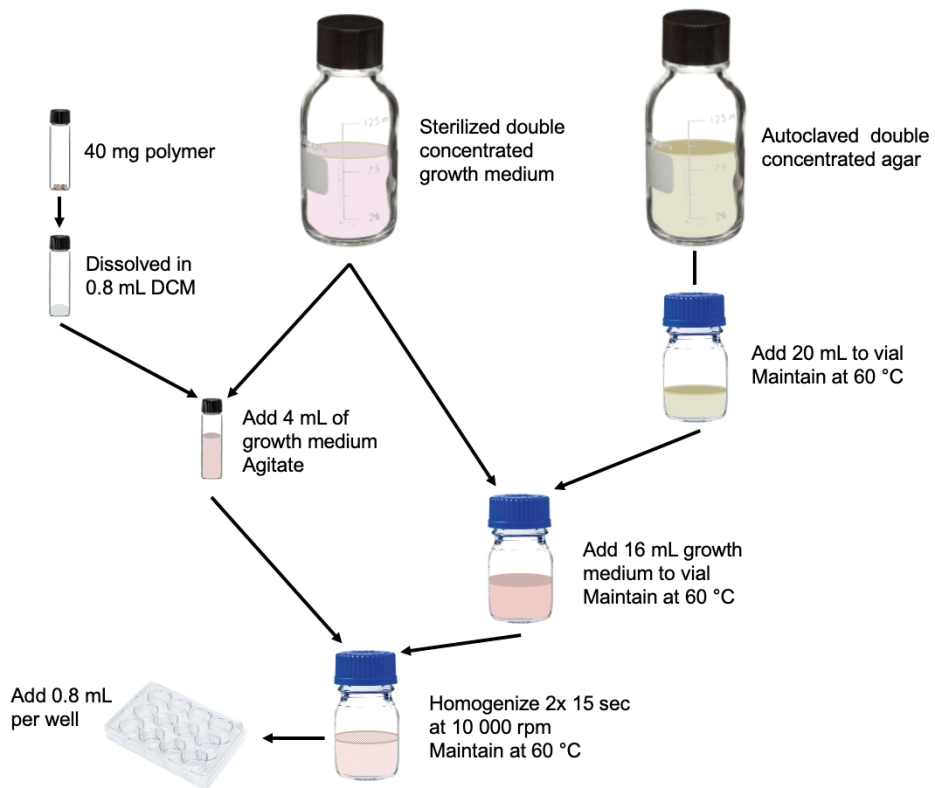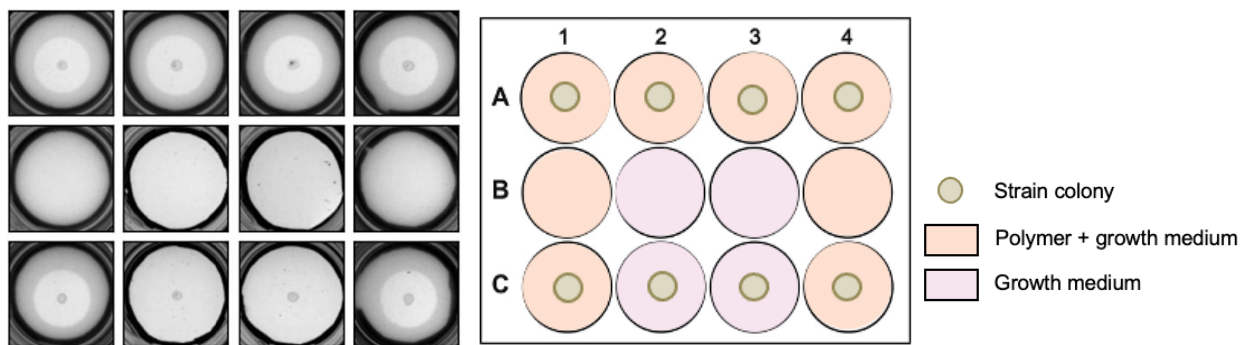

Figure S4. Biodegradation sample making process.

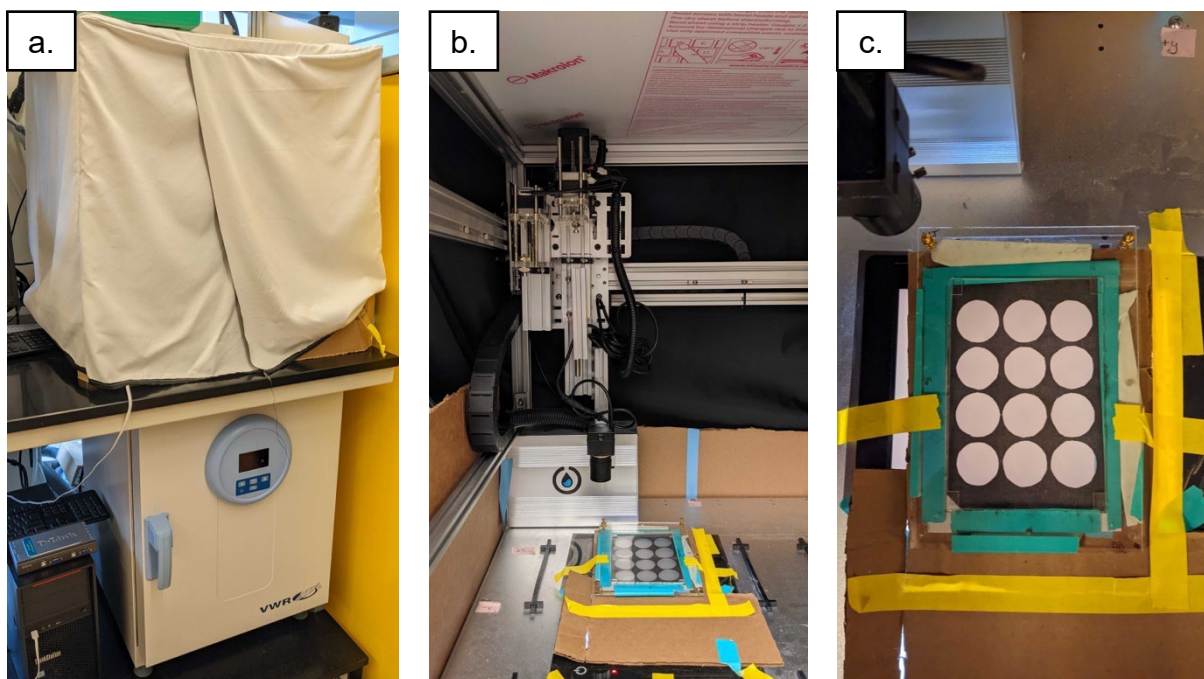**Figure S5.** Clear zone test sample: 12 well plate with controls and replicates.

Figure S6. Biodegradation monitoring robot setup. a. Opentrons OT-1 robot with light block cover with biodegradation incubator located underneath. b. Inside of the Opentrons robot, looking at the mobile arm with the attached camera able to center above each well. c. Top view of the placement holder for a 12-well plate with a blackout cutout of the wells to limit non axial incident lighting.

a.
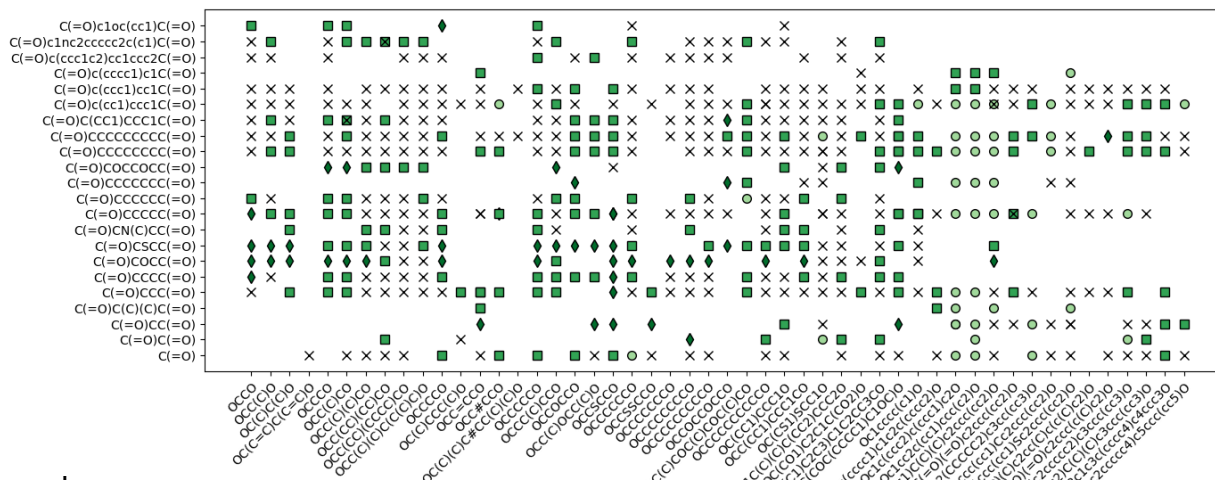
b.
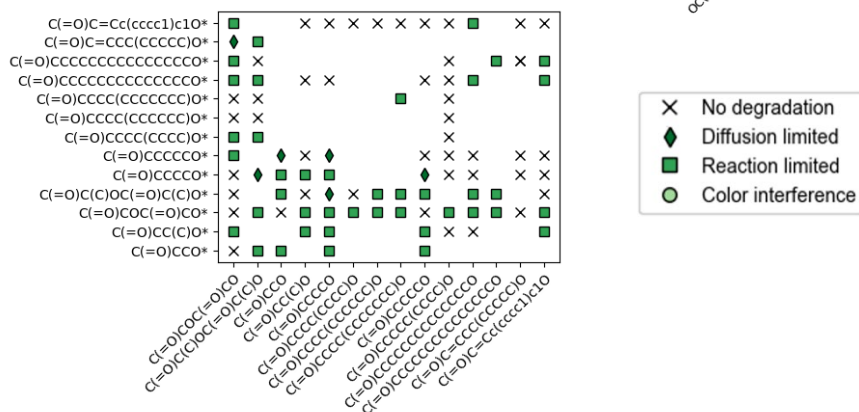
Figure S7. Biodegradation behavior of all polymers, separated by non-ring polymerization (a) and ring polymerization (b) where * indicates a ratio of 2.
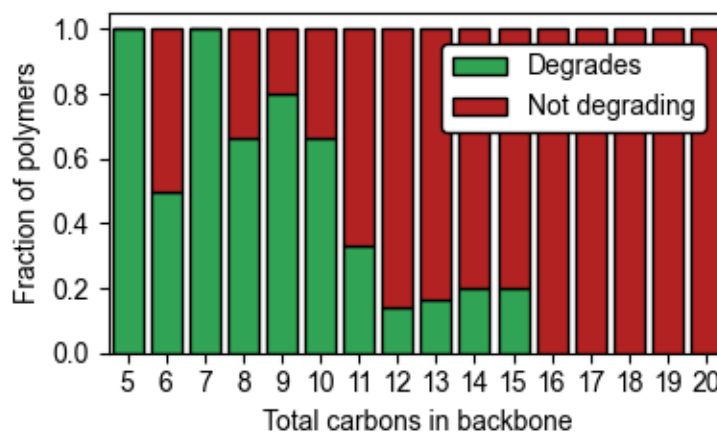

Figure S8. Biodegradation fraction of aliphatic saturated polyesters with no carbon substitutions and no side groups according to total number of carbons in the backbone of an AB repeat in the case of diacid and diol reactions.
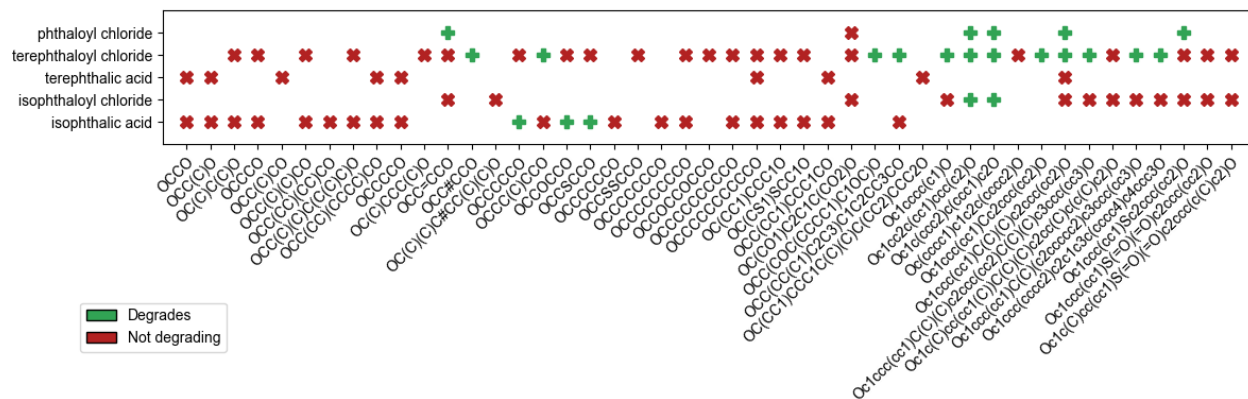
Figure S9. Biodegradation results of polymers synthesized with phthaloyl chloride, terephthaloyl chloride, terephthalic acid, isophthaloyl chloride and isophthalic acid. Phthaloyl chloride has ortho-substituted ester groups, terephthalic acid and terephthaloyl chloride have para-substituted ester groups, and isophthalic acid and isophthaloyl chloride have meta-substituted ester groups around a benzene ring.
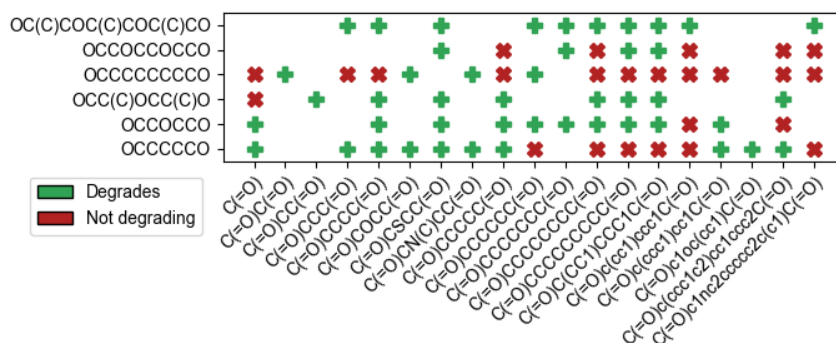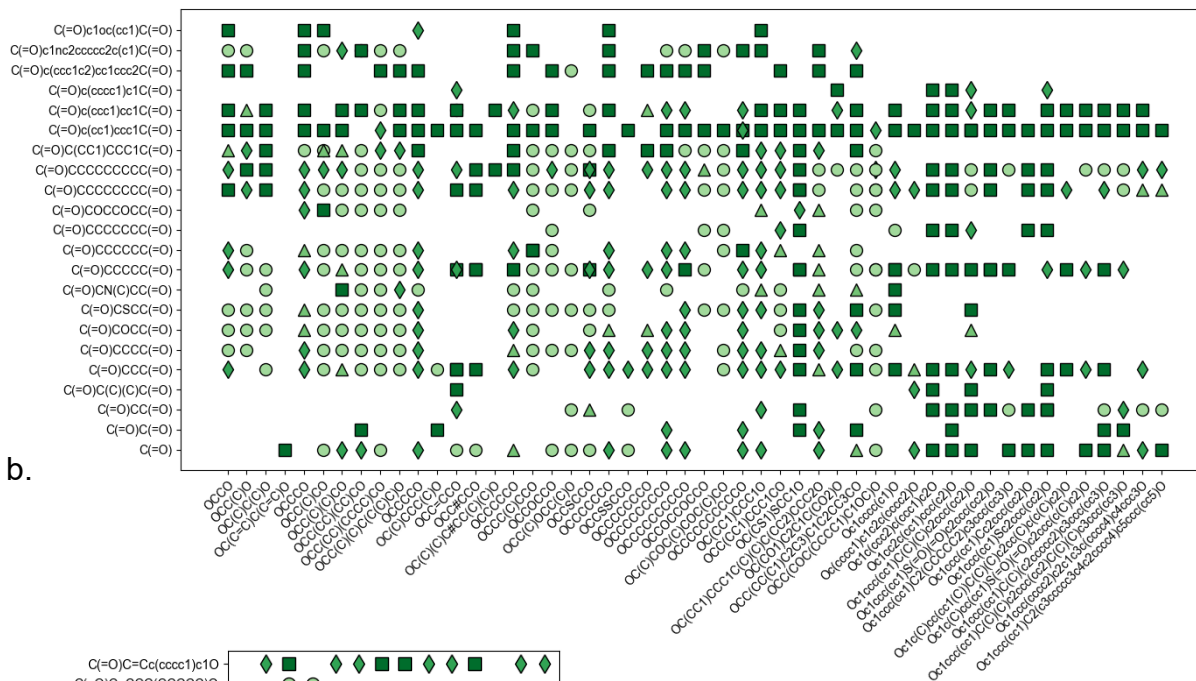

Figure S10. Biodegradation results of polymers synthesized with dipropylene glycol, tripropylene glycol and the most chemically similar diols from the polymer dataset.

Figure S11: Physical state of dataset polymers and relationship to biodegradation.
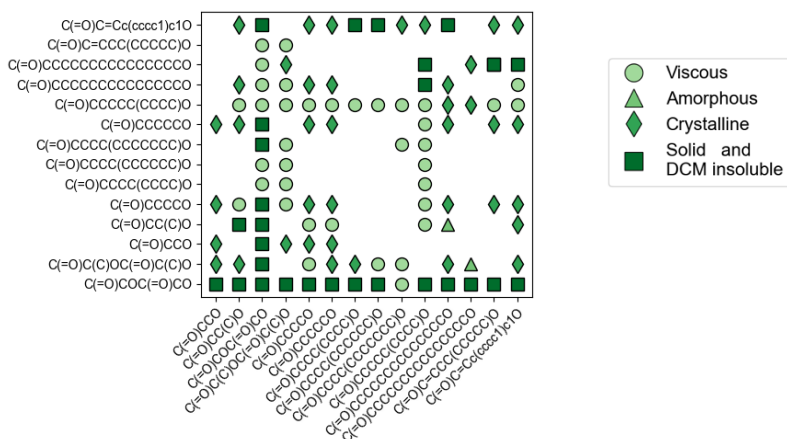
a.

b.

Figure S12. Physical state of all polymers, separated by non-ring polymerization (a) and ring polymerization (b) where * indicates a ratio of 2.

Figure S13: Dichloromethane solubility at 40 mg/mL of dataset polymers and relationship to biodegradation.
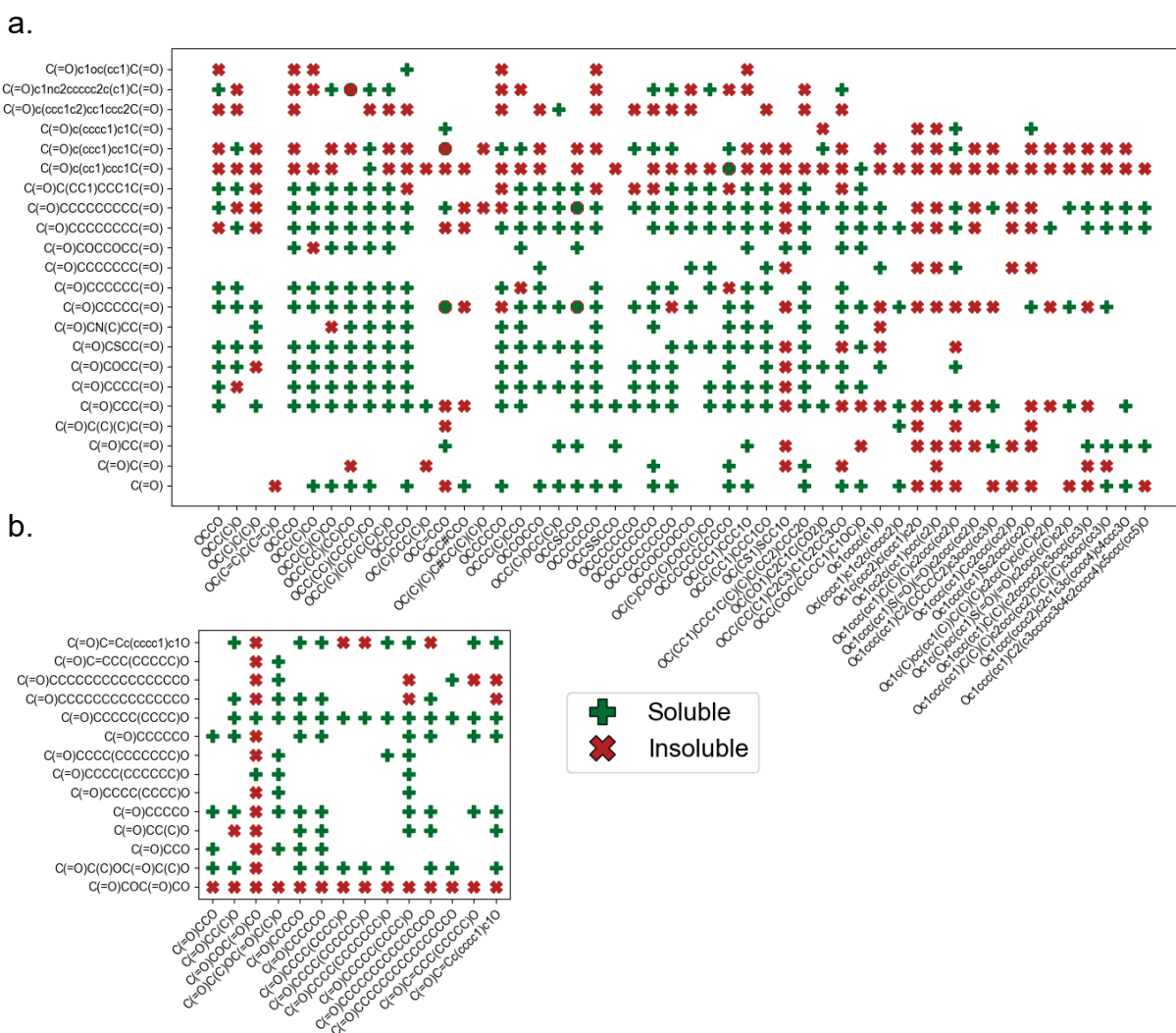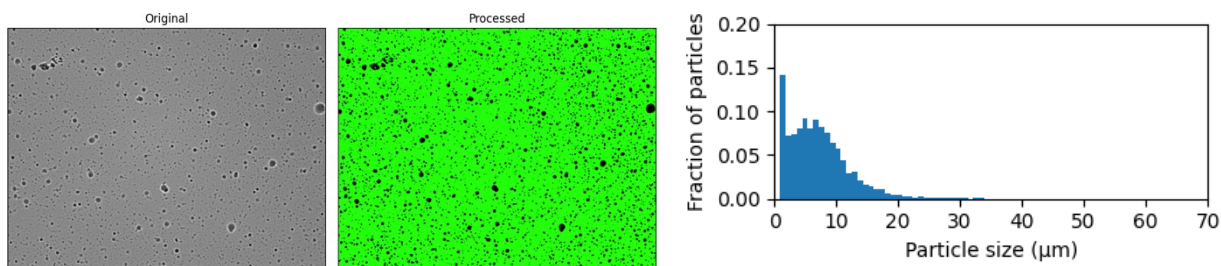
a.

b.

Figure S14. Dichloromethane solubility at 40 mg/mL of all polymers, separated by non-ring polymerization (a) and ring polymerization (b) where * indicates a ratio of 2.

- Polymer: Poly(diglycolic acid-co-ethylene glycol)

BigSMILES: {[][<]C(=O)COCC(=O)[<],[>]OCCO[>][]}
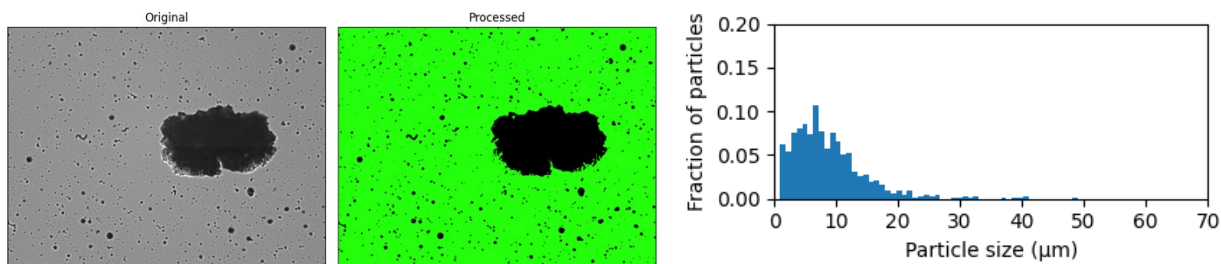DCM soluble: Yes

- Polymer: P3HB control

BigSMILES: {[] [<]OC(C)C(=O)[>][]}
DCM soluble: No

- Polymer: Poly(16-hexadecanolide-co-coumarin)

BigSMILES: {[] [<]OCCCCCCCCCCCCCCCCC(=O)[>],[<]Oc(cccc1)c1C=CC(=O)[>][]}
DCM soluble: No
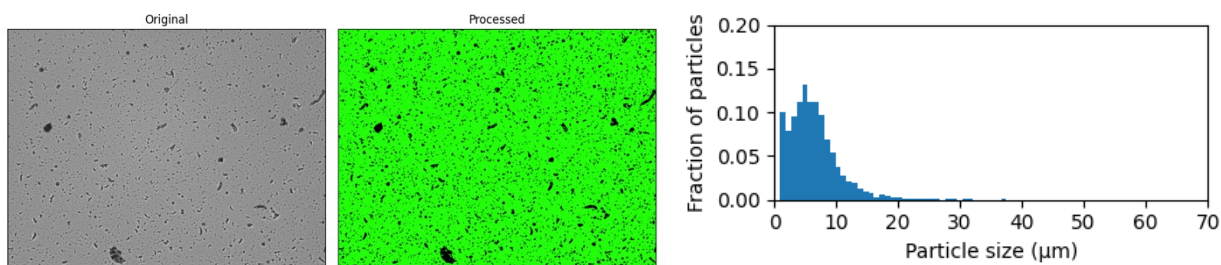
Figure S15. Particle size in agar gel quantified with image processing to find distribution of pixel counts per particle for three polymers with different DCM solubility (at a concentration of 40 mg/mL).
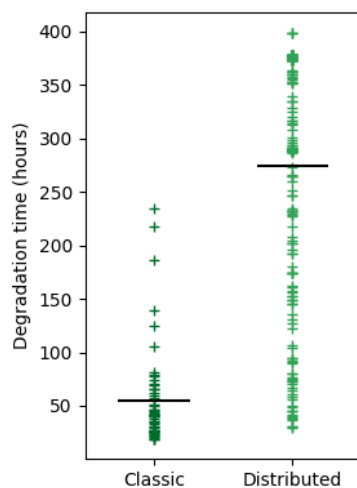
Figure S16. Average degradation time per polymer according to degradation behavior. The degradation time for each replicate was determined as the time at which OD curves between 3.7 and 7 mm distance from well center was changing.
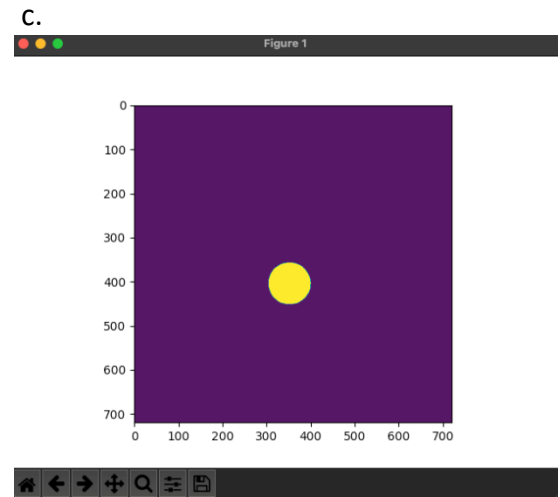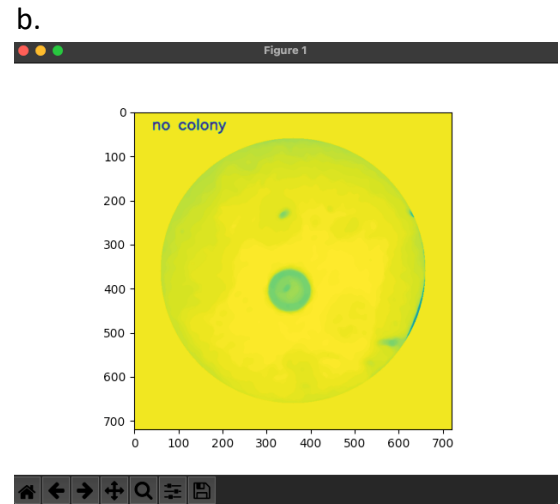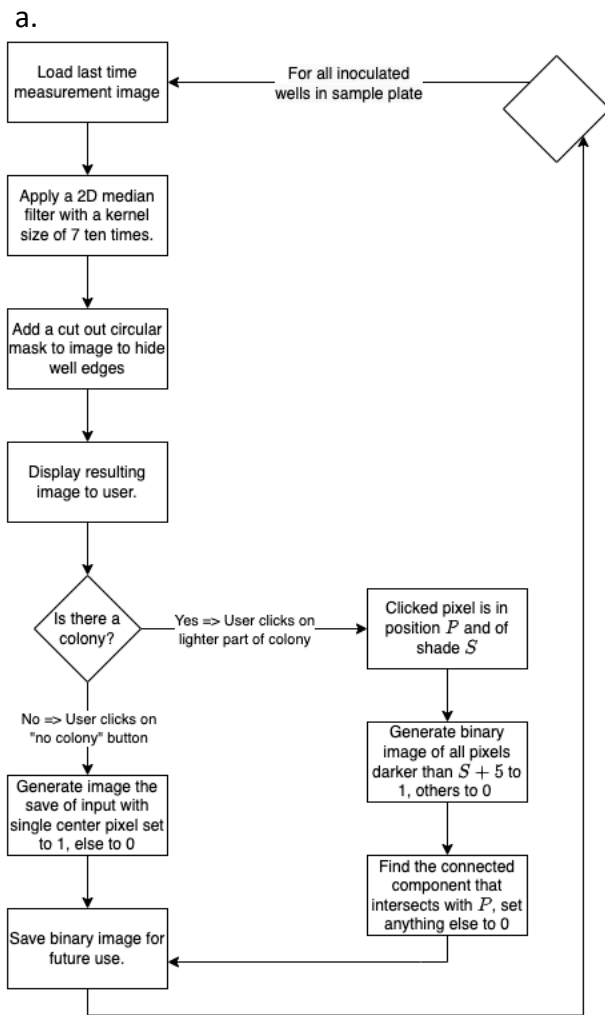
a.

```
┌─────────────────┐      For all inoculated        ◇
│ Load last time  │◄──── wells in sample plate ────◇ ◇
│ measurement     │                                ◇ ◇
│ image           │                                 ◇
└────────┬────────┘
         │
         ▼
┌─────────────────┐
│ Apply a 2D      │
│ median filter   │
│ with a kernel   │
│ size of 7 ten   │
│ times.          │
└────────┬────────┘
         │
         ▼
┌─────────────────┐
│ Add a cut out   │
│ circular mask   │
│ to image to hide│
│ well edges      │
└────────┬────────┘
         │
         ▼
┌─────────────────┐
│ Display         │
│ resulting       │
│ image to user.  │
└────────┬────────┘
         │
         ▼
```

Is there a colony? — Yes => User clicks on lighter part of colony → Clicked pixel is in position P and of shade S

No => User clicks on "no colony" button

Generate image the save of input with single center pixel set to 1, else to 0

Generate binary image of all pixels darker than $S + 5$ to 1, others to 0

Find the connected component that intersects with P, set anything else to 0

Save binary image for future use.

b.

c.

Figure S17: a. Flowchart for clear zone data extraction: finding the well colony. b. GUI of a well before the user clicks on the colony. c. GUI of a well after the user clicks on the colony.
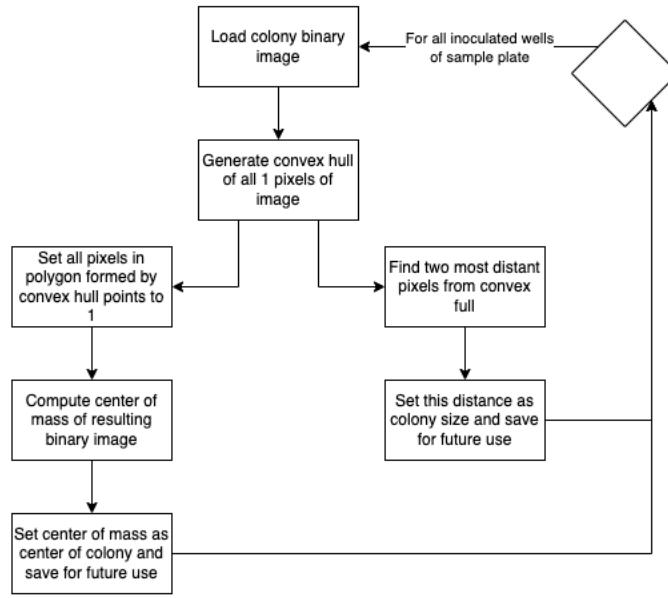
Figure S18: Flowchart for clear zone data extraction: getting well center and computing colony size.
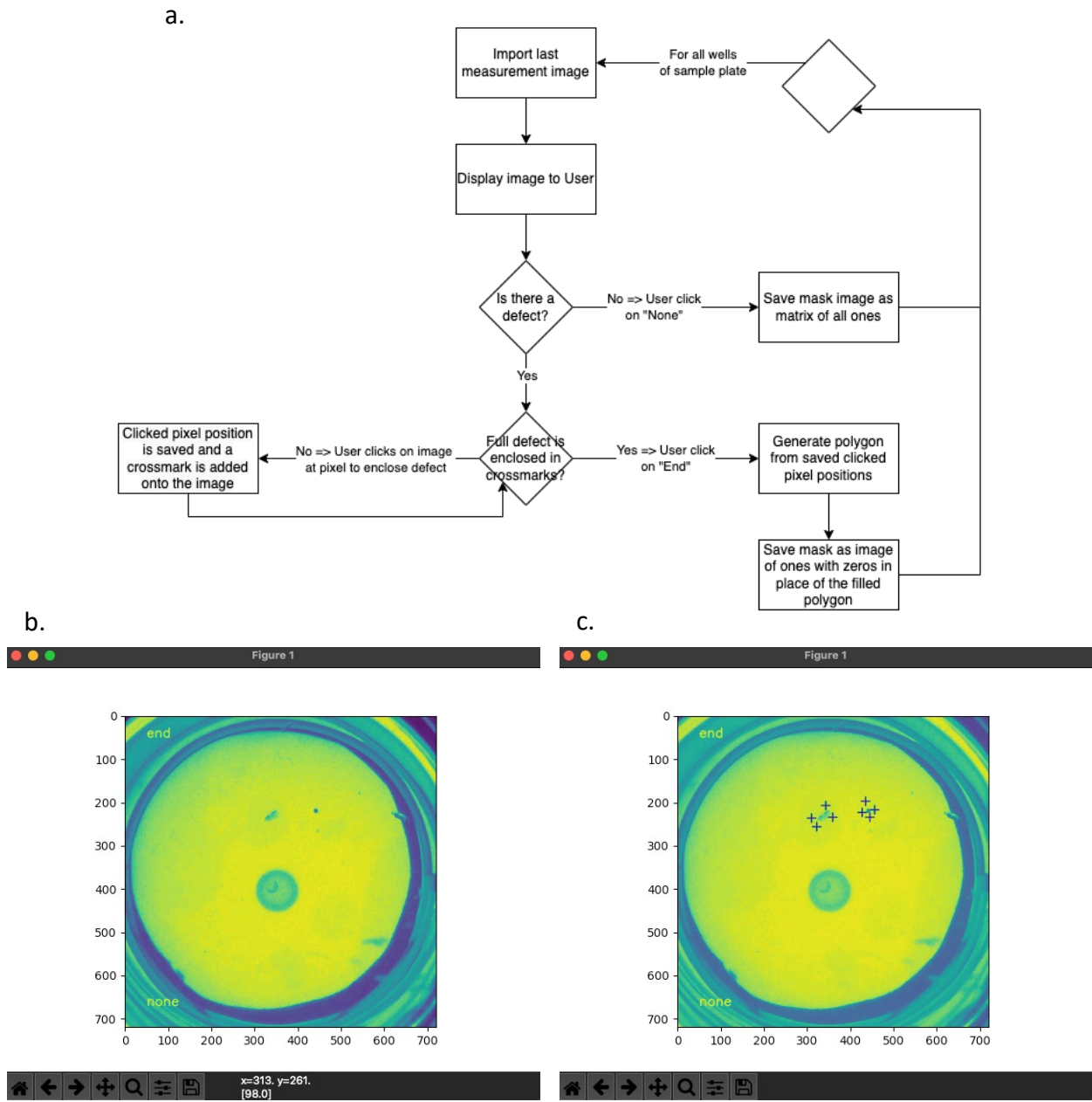
a.

b.

c.

Figure S19: a. Flowchart for clear zone data extraction: mask generation for removing sample defects. b. GUI before the user clicks to outline defects. c. GUI after the user has clicked consecutively to surround the defects.
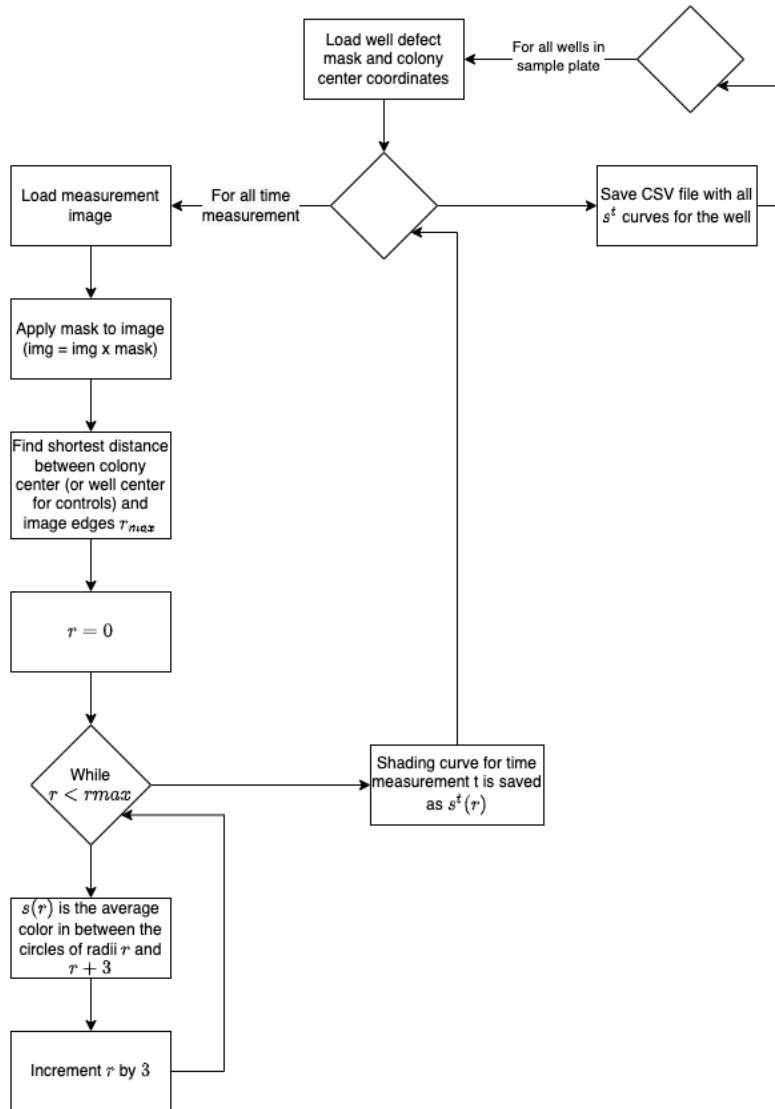
Figure S20: Flowchart for clear zone data extraction: obtain the shading curve for every well and time measurement.
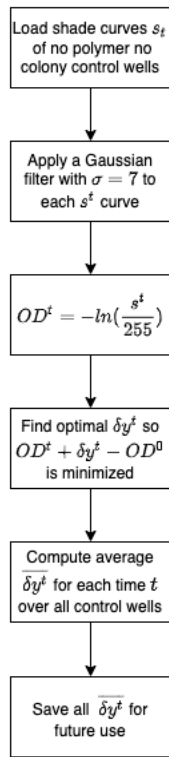
```
┌─────────────────────┐
│ Load shade curves sₜ│
│  of no polymer no   │
│ colony control wells│
└─────────────────────┘
          │
          ▼
┌─────────────────────┐
│  Apply a Gaussian   │
│ filter with σ = 7 to│
│   each sᵗ curve     │
└─────────────────────┘
          │
          ▼
```

$$OD^t = -ln(\frac{s^t}{255})$$

```
          │
          ▼
┌─────────────────────┐
│  Find optimal δyᵗ so│
│ ODᵗ + δyᵗ − OD⁰     │
│    is minimized     │
└─────────────────────┘
          │
          ▼
┌─────────────────────┐
│  Compute average    │
│ δyᵗ for each time t │
│ over all control    │
│ wells               │
└─────────────────────┘
          │
          ▼
┌─────────────────────┐
│ Save all δyᵗ for    │
│    future use       │
└─────────────────────┘
```

Figure S21: Flowchart for clear zone data extraction: compute shading curve dy adjustment from sample controls.

a. Flowchart for clear zone data extraction:

Import all shading curves $s^t(r)$

Truncate all curves to $r < 8mm$

Adjust all curves $s^t + \delta y^t => s^t$ obtained from the controls

Transform shading curves into OD:
$OD^t(r) = -log(s^t/255) - OD^0(r)$

Plot OD^t or all times in list L_t and display to user

Any outliers?

For all wells in sample plate

Save L_t of times to use for biodegradation estimation

No

Yes

User clicks on the outlier curve $OD^{t_{outlier}}$

Remove $t_{outlier}$ from L_t

b.

c.

Figure S22: a. Flowchart for clear zone data extraction: clean out time measurement outliers. b. GUI of the OD curves of a well before any time measurement is cleaned out. c. GUI of the OD curves after the user clicked on the time measurement that was a clear outlier.
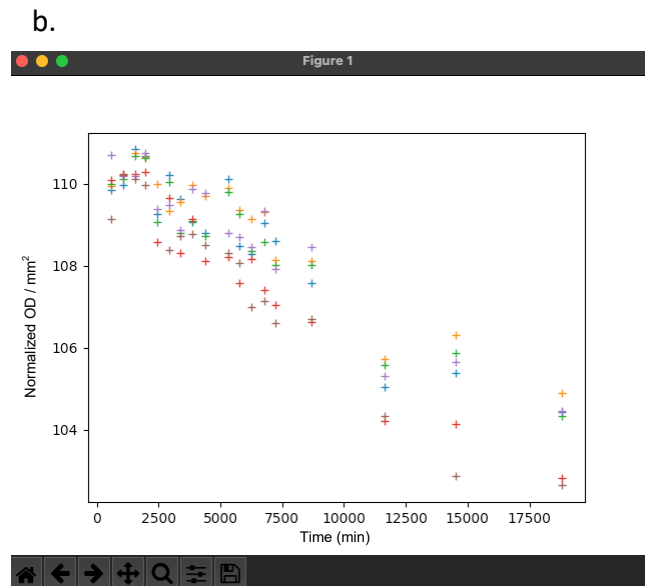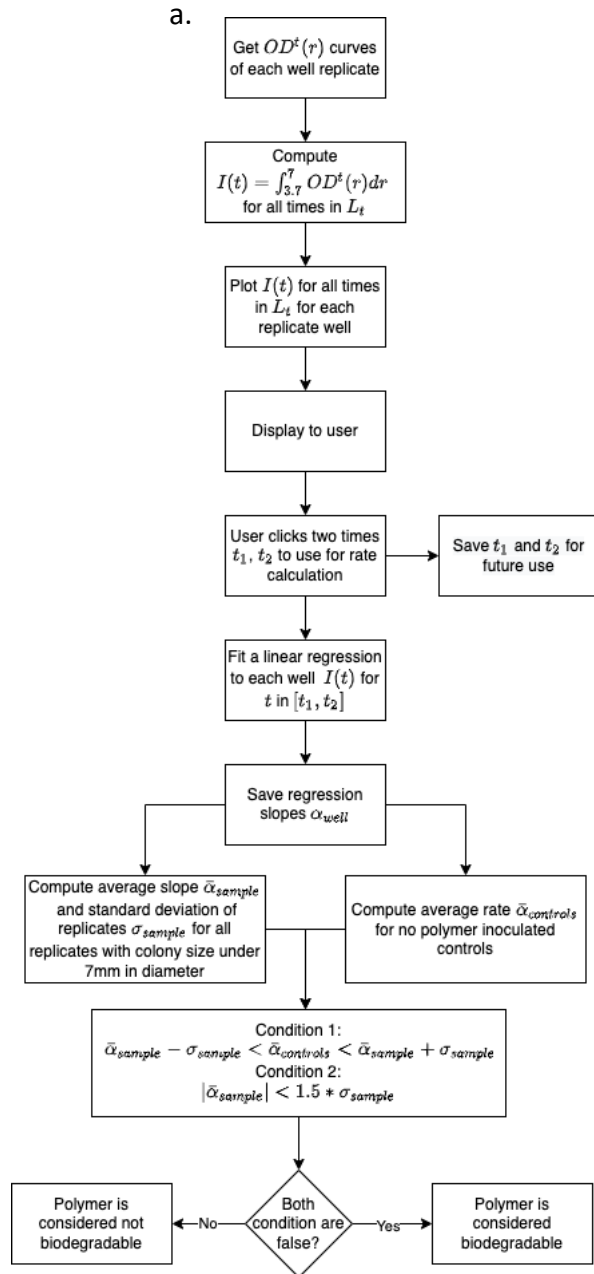
a. Flowchart

- Get $OD^t(r)$ curves of each well replicate
- Compute $I(t) = \int_{3.7}^{7} OD^t(r)dr$ for all times in L_t
- Plot $I(t)$ for all times in L_t for each replicate well
- Display to user
- User clicks two times t_1, t_2 to use for rate calculation → Save t_1 and t_2 for future use
- Fit a linear regression to each well $I(t)$ for t in $[t_1, t_2]$
- Save regression slopes α_{well}
- Compute average slope $\bar{\alpha}_{sample}$ and standard deviation of replicates σ_{sample} for all replicates with colony size under 7mm in diameter
- Compute average rate $\bar{\alpha}_{controls}$ for no polymer inoculated controls
- Condition 1: $\bar{\alpha}_{sample} - \sigma_{sample} < \bar{\alpha}_{controls} < \bar{\alpha}_{sample} + \sigma_{sample}$
  Condition 2: $|\bar{\alpha}_{sample}| < 1.5 * \sigma_{sample}$
- Both condition are false? — No → Polymer is considered not biodegradable
- Yes → Polymer is considered biodegradable

Figure S23: a. Flowchart for clear zone data extraction: get degradation rate to determine biodegradability. b. GUI of the plotted integration value of all the replicates for one polymer, where the user clicks outside of the time points they wish to include in the calculation. In this case the linear trend lasts for the full set of measurements; therefore all datapoints will be included.
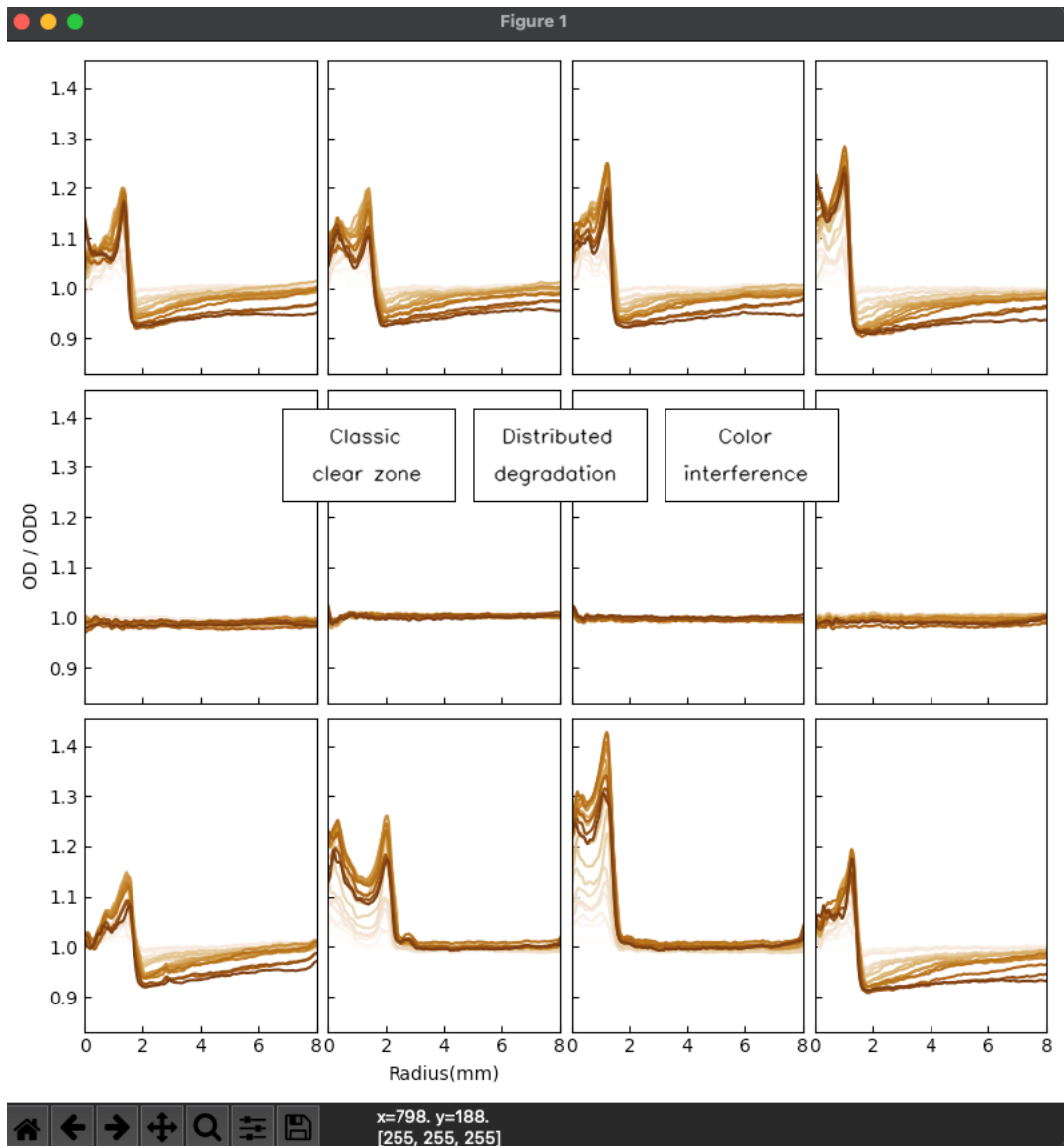
Figure S24: GUI of a polymer sample with all the OD curves plotted for each well on the plate. The user decides what behavior the degradation is like. In this case, the OD curves are progressively reaching lower values and have no neat trend like a classic clear zone; therefore it is a distributed degradation behavior.
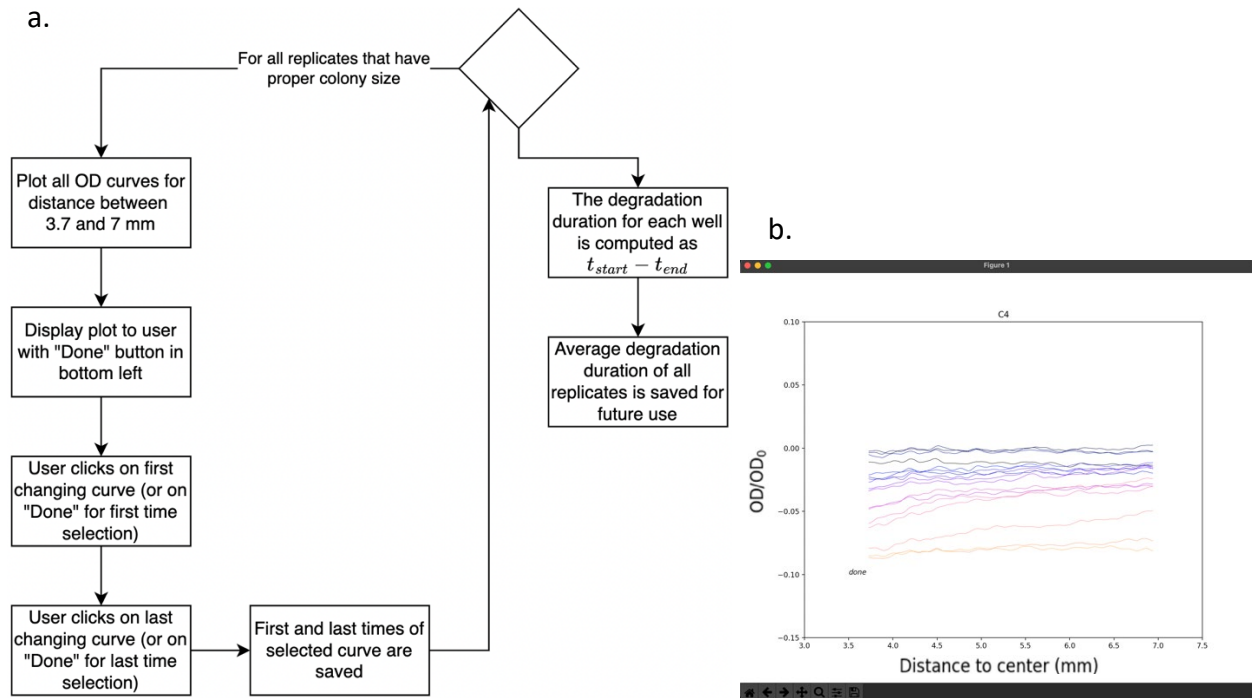
Figure S25: a. Degradation duration flowchart. b. GUI displayed to the user for first and last changing curve selection.
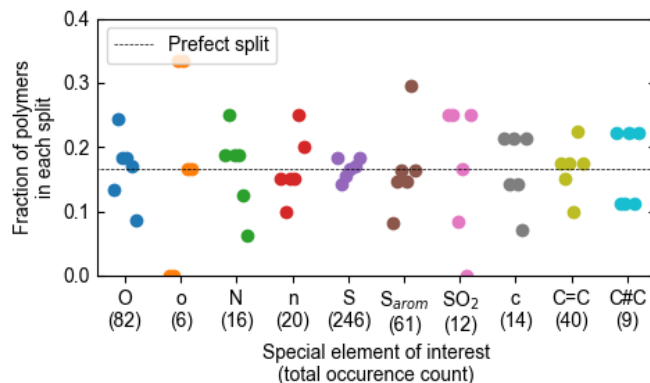
Figure S26: Distribution of special elements for the full data 6-way split for machine learning training, testing and validation. The data was split to have approximately equal amounts of polymers containing oxygen, nitrogen, sulfur, aromatic rings, double bonded carbons and triple bonded carbons.
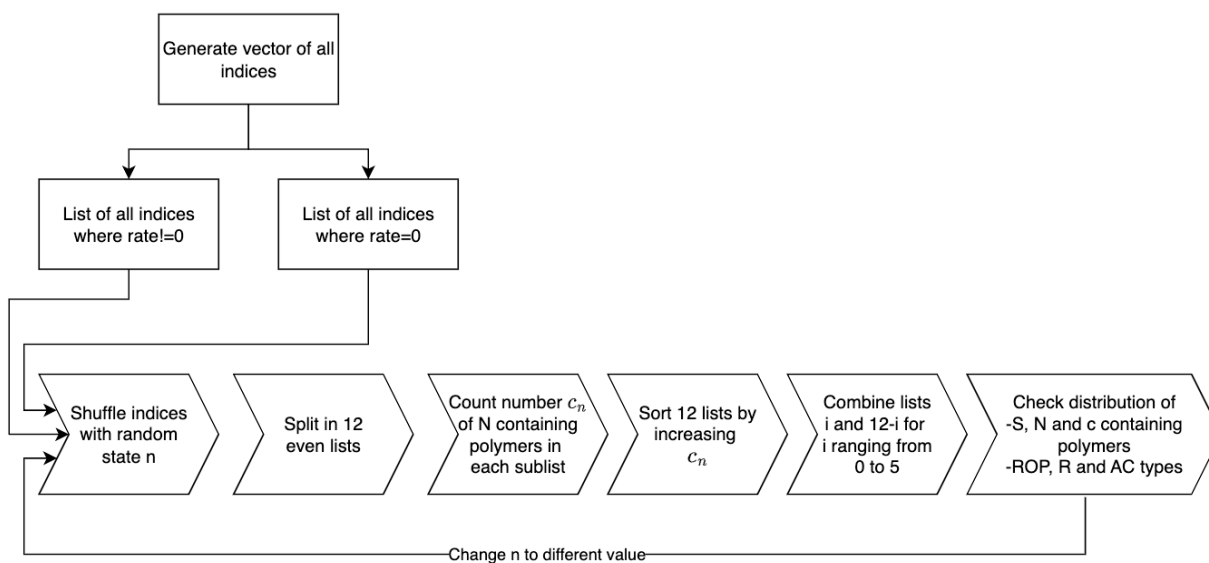

Figure S27: Data splitting flowchart for machine learning training, testing and validation sets.
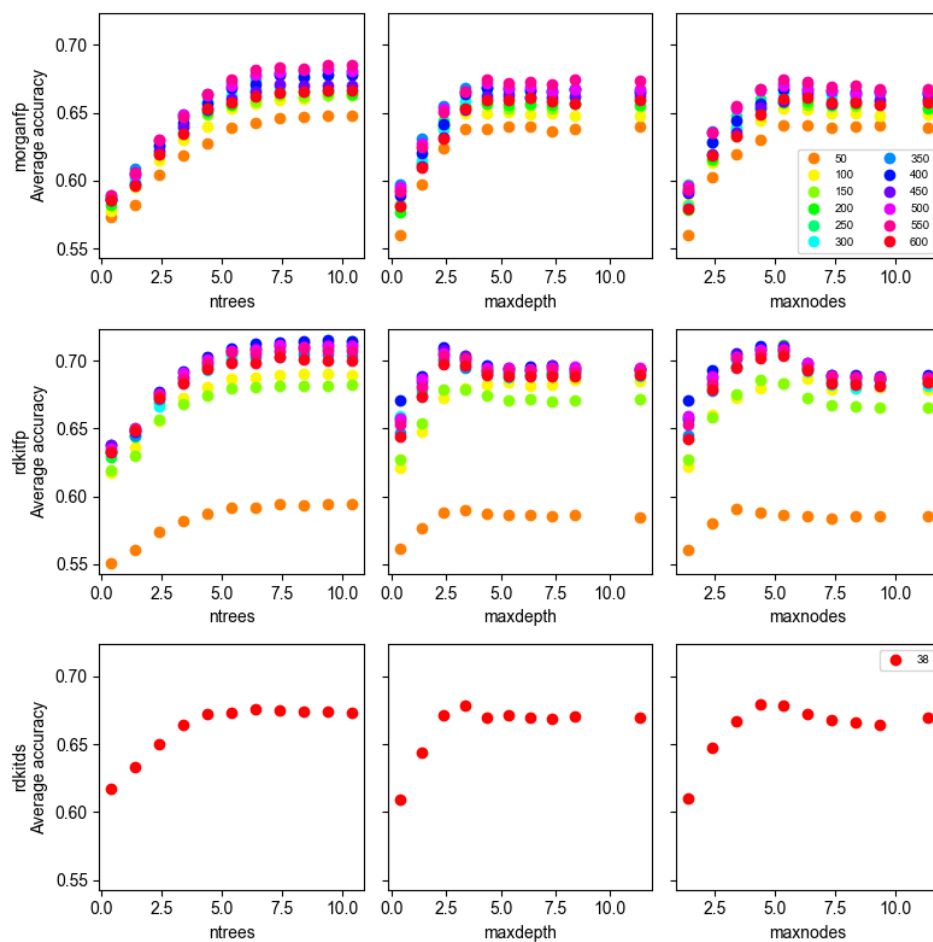
Figure S28: Random Forest hyperparameter optimization for the full dataset using only chemical description as features. Optimization is done for the number of trees, the maximum depth and the maximum number of nodes for the three chemical description vectorizations (morgan fingerprinting, RDKit fingerprinting and RDKit descriptors). The legend is the size of the vector before feature reduction.
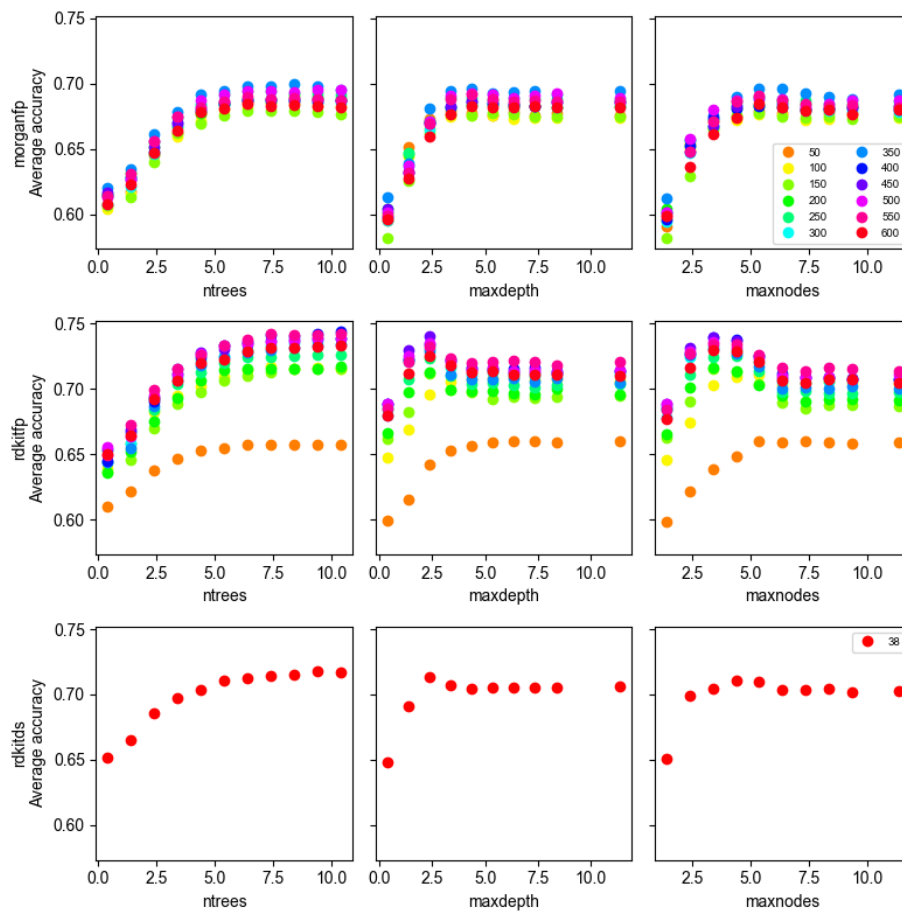
Figure S29: Random Forest hyperparameter optimization for the sub dataset of all polymers with determined physical state using chemical description and physical state as features. Optimization is done for the number of trees, the maximum depth and the maximum number of nodes for the three chemical description vectorizations (morgan fingerprinting, RDKit fingerprinting and RDKit descriptors). The legend is the size of the vector before feature reduction.
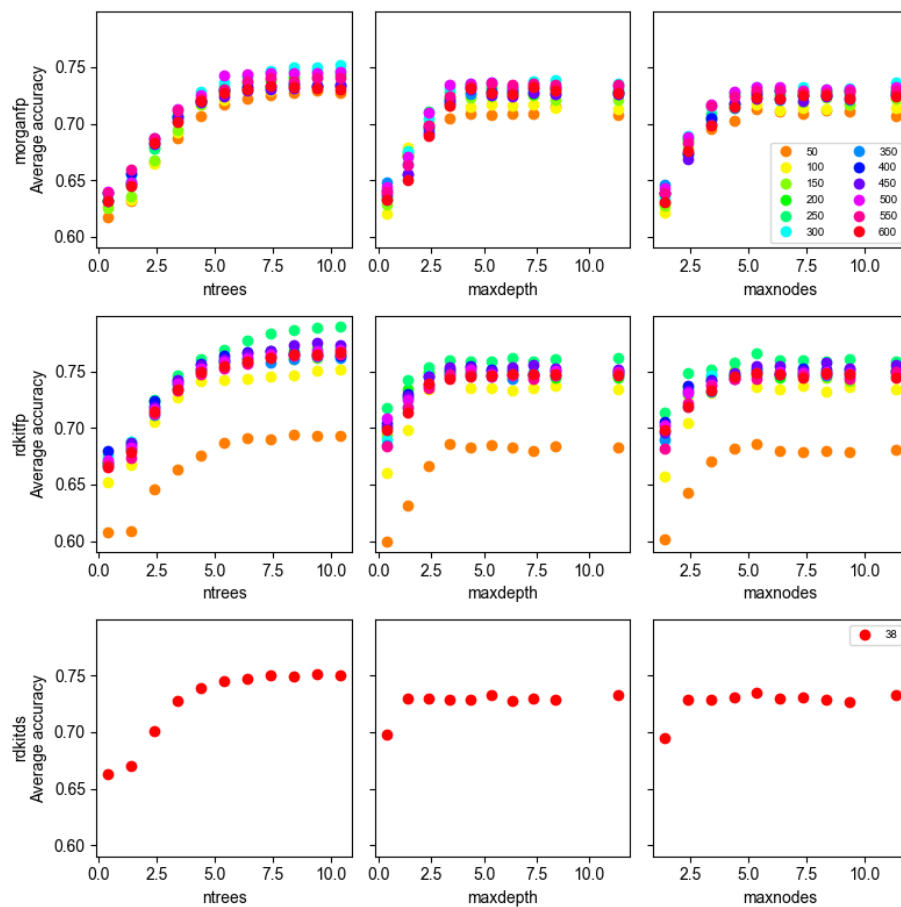
Figure S30: Random Forest hyperparameter optimization for the sub dataset of all polymers with determined molecular weight using chemical description and GPC data as features. Optimization is done for the number of trees, the maximum depth and the maximum number of nodes for the three chemical description vectorizations (Morgan fingerprinting, RDKit fingerprinting and RDKit descriptors). The legend is the size of the vector before feature reduction.
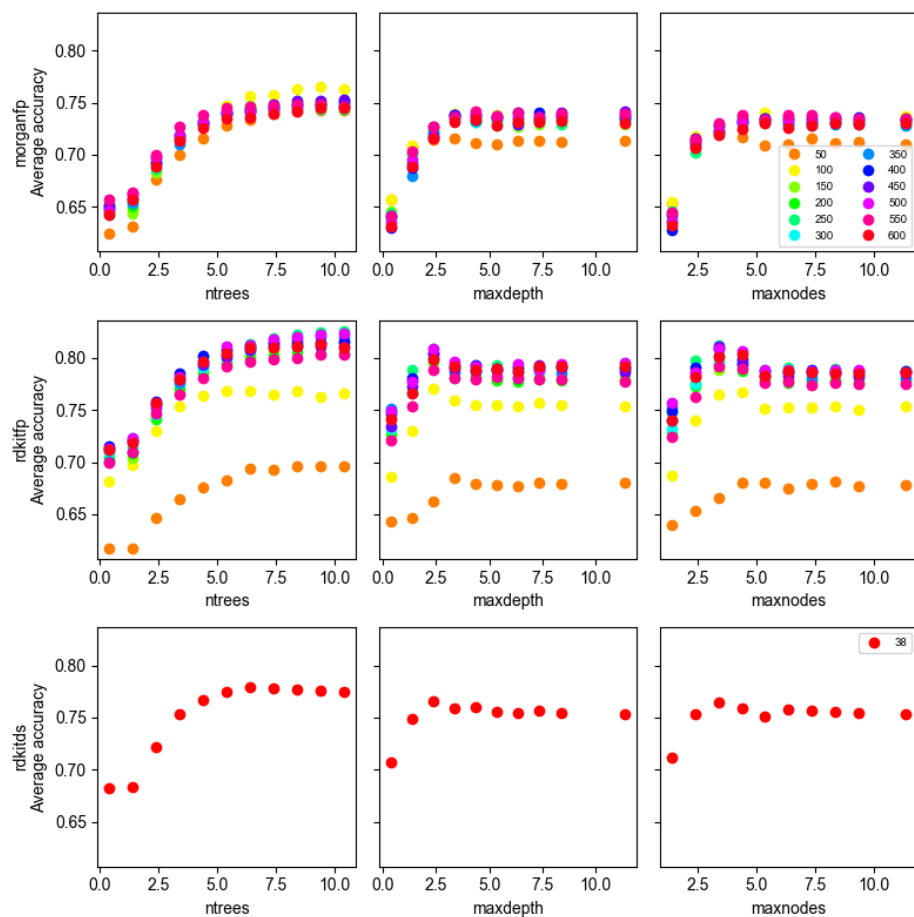
Figure S31: Random Forest hyperparameter optimization for the sub dataset of all polymers with determined molecular weight and physical state using chemical description, GPC data and physical state as features. Optimization is done for the number of trees, the maximum depth and the maximum number of nodes for the three chemical description vectorizations (Morgan fingerprinting, RDKit fingerprinting and RDKit descriptors). The legend is the size of the vector before feature reduction.
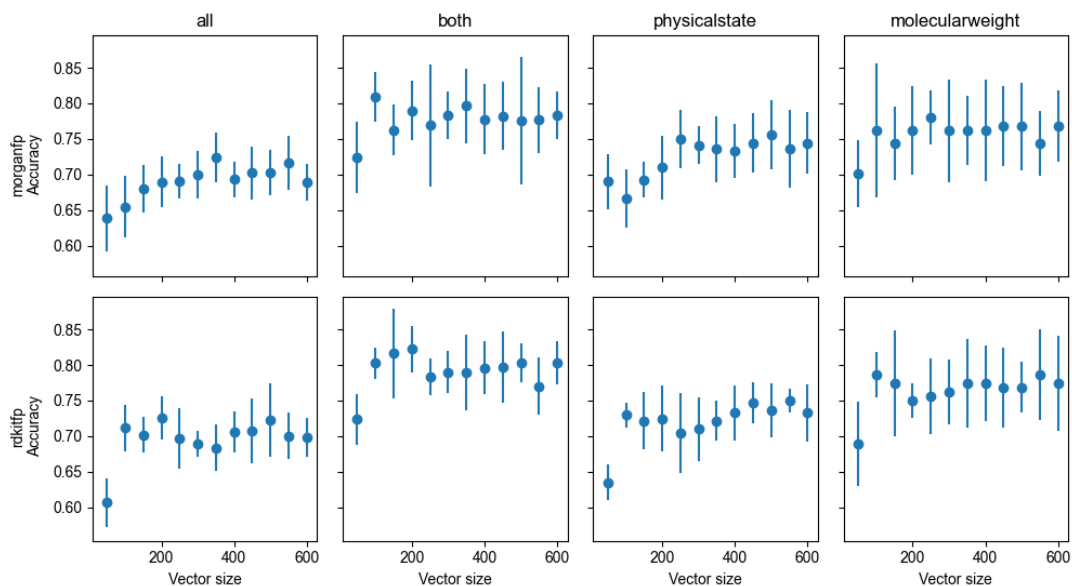
Figure S32: Random Forest classification vector size optimization for all datasets with corresponding features. Optimization is done for the three chemical description vectorizations Morgan fingerprinting and RDKit fingerprinting.

Figure S33: Logistic classification vector size optimization for all datasets with corresponding features. Optimization is done for the three chemical description vectorizations Morgan fingerprinting and RDKit fingerprinting.
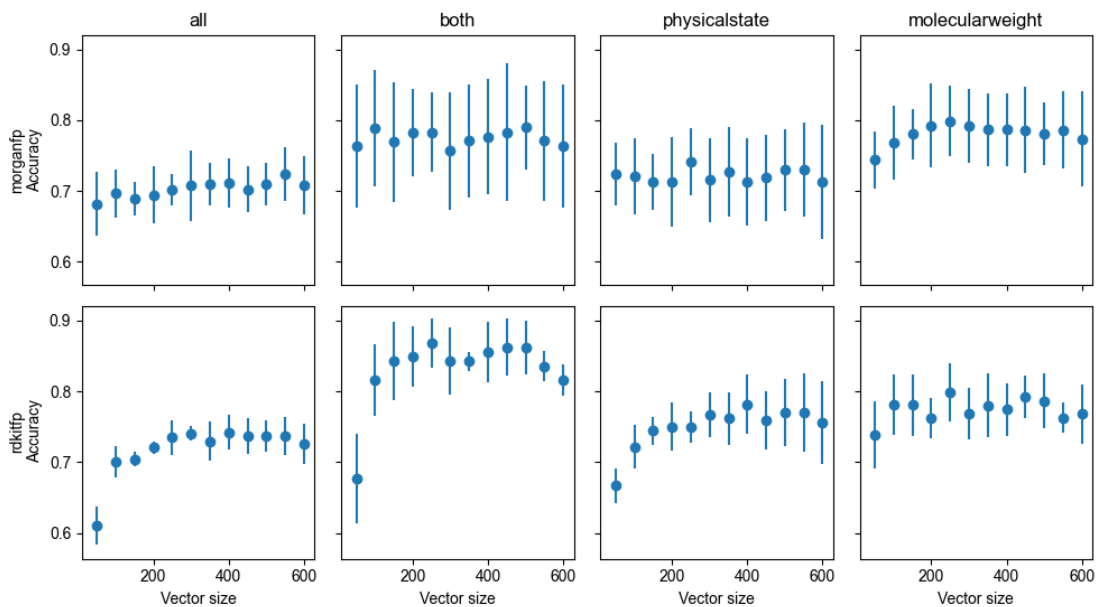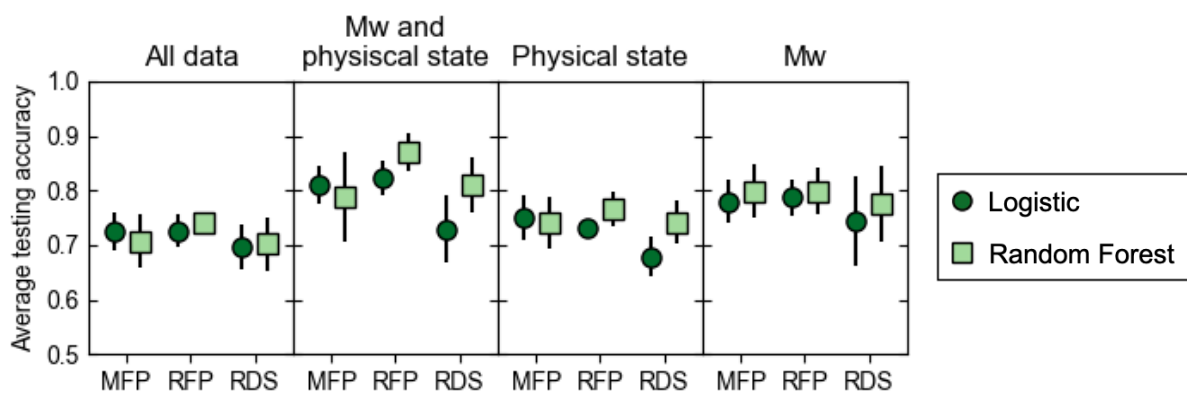
Figure S34: Testing accuracy for each dataset with corresponding feature vectors, for optimized hyperparameters for each model used and each vectorization scheme.
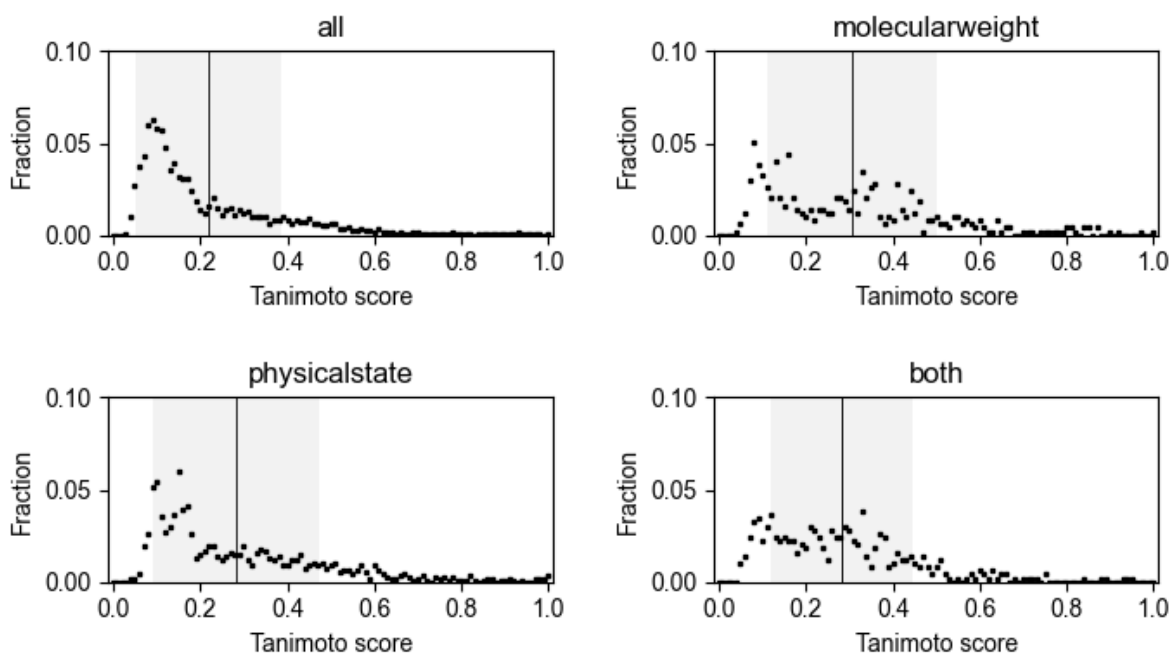

Figure S35: Chemical diversity for the different data sets used in machine learning modeling of biodegradability. Plotted is the fraction polymers in each dataset with given Tanimoto score. The vertical black line makes the average of the distribution and the grey zone is of a width of two standard deviations.
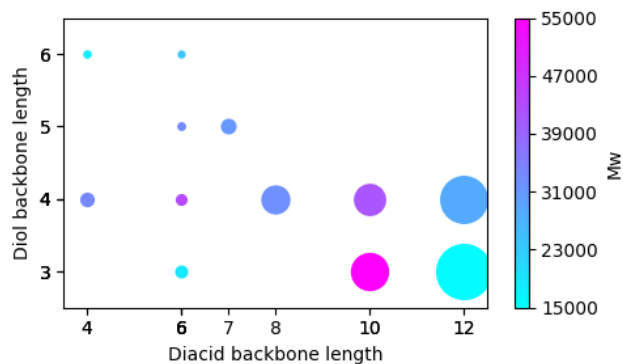
Figure S36: Degradation rate according to polymer repeat unit length of the diol and diacid in Herzog *et. al.*'s study(18).
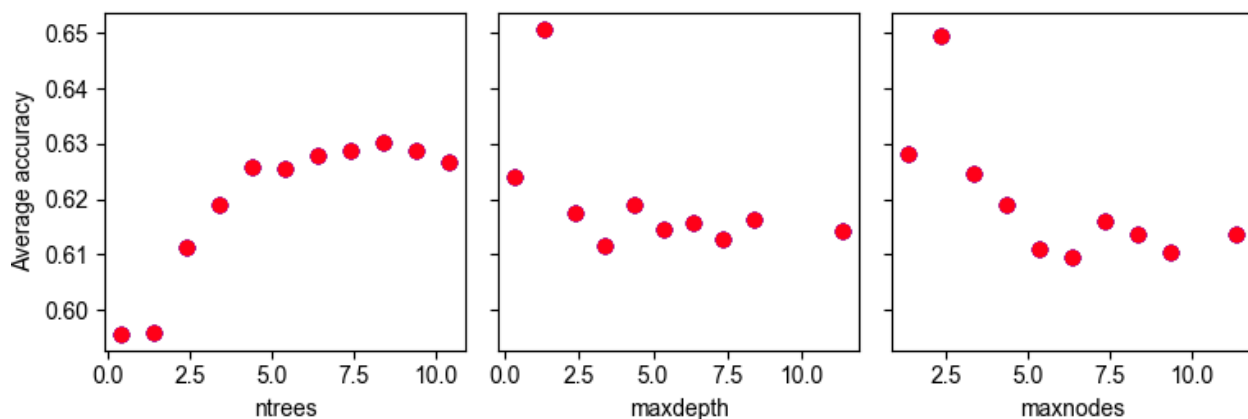
Figure S37: Random Forest hyperparameter optimization for the sub dataset of GPC data and physical state as features, without chemical descriptors as input. Optimization is done for the number of trees, the maximum depth and the maximum number of nodes.

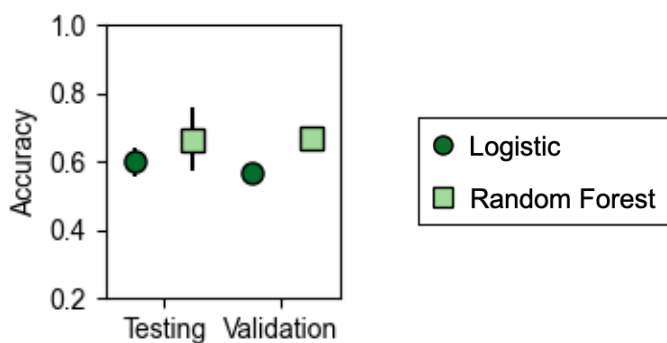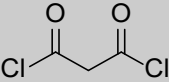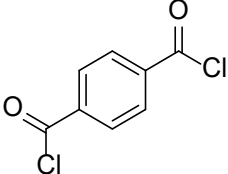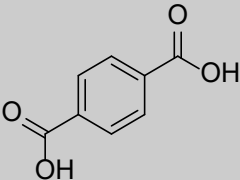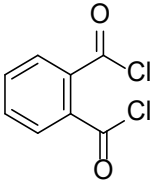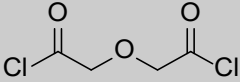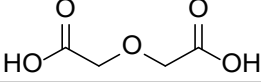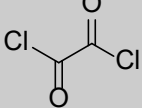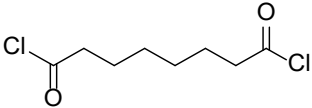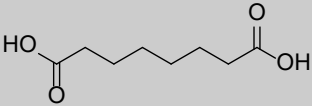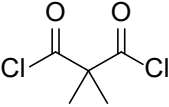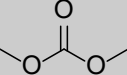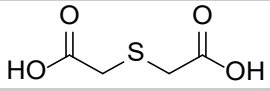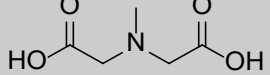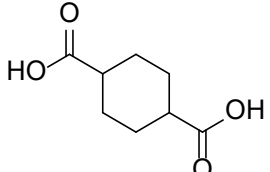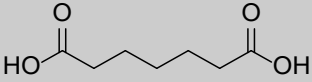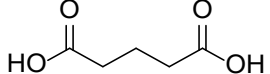**Figure S38**: Testing and validation accuracy for the sub dataset of GPC data and physical state as features without chemical descriptors as input, for optimized hyperparameters for each model used.
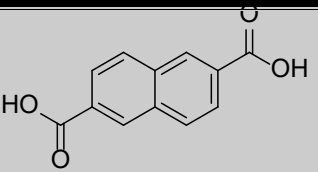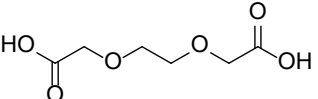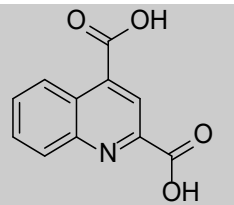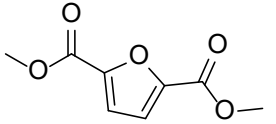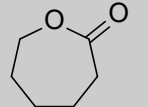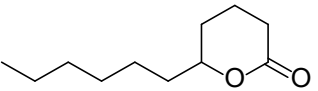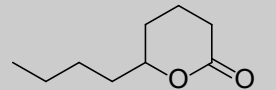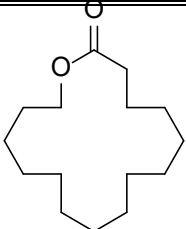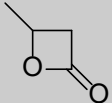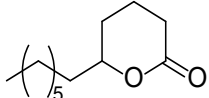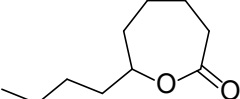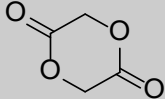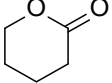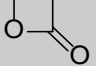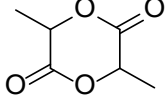
Table S1: Details of Monomers included in the Library.
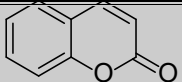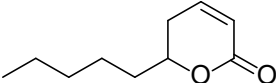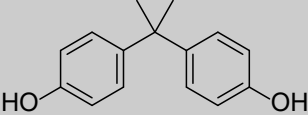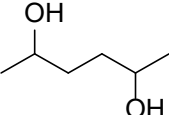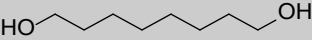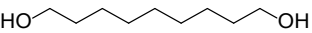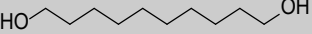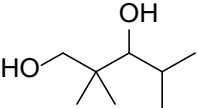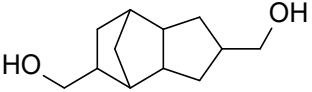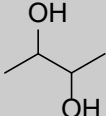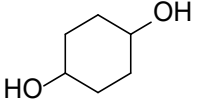
Monomer Name	Monomer Structure	SMILES	Number of Representations in Library	Represented Chemical Functionalities
Malonyl Chloride		[Cl]C(=O)CC(=O)[Cl]	6	
Terephthaloyl Chloride		[Cl]C(=O)c1ccc(cc1)C(=O)[Cl]	37	Aromatic
Terephthalic Acid		OC(=O)c1ccc(cc1)C(=O)O	6	Aromatic
Phthaloyl chloride		[Cl]C(=O)c(cccc1)c1C(=O)[Cl]	7	Aromatic
Diglycolyl Chloride		[Cl]C(=O)COC(=O)[Cl]	11	Oxygen
Diglycolic Acid		OC(=O)COC(=O)O	27	Oxygen
Oxalyl Chloride		[Cl]C(=O)C(=O)[Cl]	10	

Monomer Name	Monomer Structure	SMILES	Number of Representations in Library	Represented Chemical Functionalities
Sebacoyl Chloride		[Cl]C(=O)CCCCCCCC(=O)[Cl]	20	
Sebacic Acid		OC(=O)CCCCCCCC(=O)O	25	
Succinyl Chloride		[Cl]C(=O)CCC(=O)[Cl]	14	
Succinic Acid		OC(=O)CCC(=O)O	28	
Isophthaloyl chloride		[Cl]C(=O)c(ccc1)cc1C(=O)[Cl]	15	Aromatic
Isophthalic Acid		OC(=O)c(ccc1)cc1C(=O)O	22	Aromatic
Adipoyl Chloride		[Cl]C(=O)CCCC(=O)[Cl]	17	
Adipic Acid		OC(=O)CCCC(=O)O	22	
Azelaoyl Chloride		[Cl]C(=O)CCCCCCC(=O)[Cl]	17	
Azelaic Acid		OC(=O)CCCCCCC(=O)O	25	
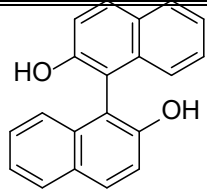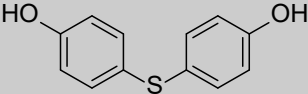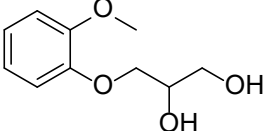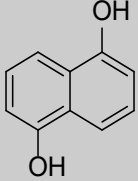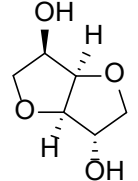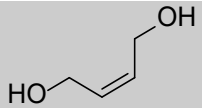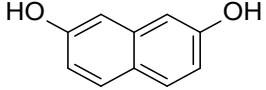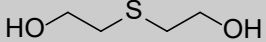
Monomer Name	Monomer Structure	SMILES	Number of Representations in Library	Represented Chemical Functionalities
Suberoyl Chloride		[Cl]C(=O)CCCCCCC(=O)[Cl]	7	
Suberic Acid		OC(=O)CCCCCCC(=O)O	4	
Dimethylmalonyl Chloride		[Cl]C(=O)C(C)(C)C(=O)[Cl]	5	
Dimethyl Carbonate		COC(=O)OC	34	
2,2′-Thiodiacetic acid		OC(=O)CSCC(=O)O	28	Sulfur
[(Carboxymethyl)(methyl)amino]acetic acid		OC(=O)CN(C)CC(=O)O	16	Nitrogen
1,4-Cyclohexanedicarboxylic acid		OC(=O)C(CC1)CCC1C(=O)O	28	Ring
Pimelic Acid		OC(=O)CCCCC(=O)O	22	
Glutaric Acid		OC(=O)CCCC(=O)O	26	

Monomer Name	Monomer Structure	SMILES	Number of Representations in Library	Represented Chemical Functionalities
2,6-Naphthalenedicarboxylic Acid		OC(=O)c(ccc1c2)cc1ccc2C(=O)O	17	Aromatic
2,2′-[ethylenebis(oxy)] bisacetic acid		OC(=O)COCCOCC(=O)O	13	Oxygen
quinoline-2,4-dicarboxylic acid		OC(=O)c1nc2ccccc2c(c1)C(=O)O	19	Nitrogen, Aromatic
2,5-furandicarboxylic acid methyl ester		C(=O)c(o1)ccc1C(=O)	7	Oxygen, Aromatic
ε-Caprolactone		O1CCCCCC1(=O)	19	
Undecanoic δ-lactone		O1C(CCCCCC)CCCC1(=O)	7	
δ-nonalactone		O1C(CCCC)CCCC1(=O)	7	

Monomer Name	Monomer Structure	SMILES	Number of Representations in Library	Represented Chemical Functionalities
pentadecanolide		O1CCCCCCCCCCCCCC C1(=O)	16	
β-butyrolactone		O1C(C)CC1(=O)	14	
5-Dodecanolide		O1C(CCCCCCC)CCCC1(=O)	8	
16-hexadecanolide		O1CCCCCCCCCCCCCC CC1(=O)	9	
ε-Decalactone		O1C(CCCC)CCCCC1(=O)	23	
glycolide		O1CC(=O)OCC1(=O)	27	
δ-Valerolactone		O1CCCCC1(=O)	18	
β-propiolactone		O1CCC1(=O)	9	
lactide		O1C(C)C(=O)OC(C)C1(= O)	21	

Monomer Name	Monomer Structure	SMILES	Number of Representations in Library	Represented Chemical Functionalities
Coumarin		O1c(cccc2)c2C=CC1(=O)	19	Aromatic, Double Bond
Massoia Lactone		O1C(CCCCC)CC=CC1(O)	9	Double Bond
Bisphenol A		Oc1ccc(cc1)C(C)(C)c2ccc(cc2)O	13	Aromatic
2,5-hexanediol (+isomers)		OC(C)CCC(C)O	3	
1,8-octanediol		OCCCCCCCCO	15	
1,9-nonanediol		OCCCCCCCCCO	14	
1,10-decanediol		OCCCCCCCCCCO	15	
2,2,4-Trimethyl-1,3-pentanediol		OCC(C)(C)C(C(C)C)O	15	
2,2-Dimethyl-1,3-propanediol		OCC(C)(C)CO	15	
4,8-Bis(hydroxymethyl)tricyclo[5.2.1.02,6]decane		OCC(CC(C1)C2C3)C1C2CC3CO	17	Ring
2,3-Butanediol		OC(C)C(C)O	10	
1,4-Cyclohexanediol		OC(CC1)CCC1O	16	Ring

Monomer Name	Monomer Structure	SMILES	Number of Representations in Library	Represented Chemical Functionalities
Diethylene Glycol		OCCOCCO	21	Oxygen
Triethylene Glycol		OCCOCCOCCO	9	Oxygen
4,4′-Sulfonylbis(2-methylphenol)		Oc1c(C)cc(cc1)S(=O)(=O)c2ccc(c(C)c2)O	6	Sulfur, Aromatic
2-Hydroxyethyl disulfide		OCCSSCCO	4	Sulfur
1,3-Bis[2-(4-hydroxyphenyl)-2-propyl]benzene		Oc1ccc(cc1)C(C)(C)c2ccc(cc2)C(C)(C)c3ccc(cc3)O	8	Aromatic
4,4′-(α-Methylbenzylidene)bisphenol		Oc1ccc(cc1)C(C)(c2ccccc2)c3ccc(cc3)O	9	Aromatic
4,4′-Isopropylidenebis(2,6-dimethylphenol)		Oc1c(C)cc(cc1(C))C(C)(C)c2cc(C)c(c(C)c2)O	5	Aromatic
4,4′-(9-Fluorenylidene)diphenol		Oc1ccc(cc1)C2(c3ccccc3c4c2ccccc4)c5ccc(cc5)O	5	Aromatic
4,4′-Cyclohexylidenebisphenol		Oc1ccc(cc1)C2(CCCCC2)c3cc(cc3)O	7	Aromatic, Ring

Monomer Name	Monomer Structure	SMILES	Number of Representations in Library	Represented Chemical Functionalities
(R)-(+)-1,1′-Binaphthyl-2,2′-diol		Oc1ccc(cccc2)c2c1c3c(cccc4)c4ccc3O	7	Aromatic
4,4′-Thiodiphenol		Oc1ccc(cc1)Sc2ccc(cc2)O	12	Sulfur, Aromatic
Guaiacol glyceryl ether		OCC(COC(CCCC1)C1OC)O	12	Oxygen, Ring
Naphthalene-1,5-diol		Oc1c(ccc2)c(ccc1)c2O	12	Aromatic
Dianhydro-D-glucitol		OC(C1CO1)C(C2CO2)O	6	Oxygen, Ring
cis-2-Butene-1,4-diol		OC/C=C/CO	10	Double Bond
2,7-Naphthalenediol		Oc1cc2c(cc1)ccc(c2)O	11	Aromatic
2,2′-Thiodiethanol		OCCSCCO	12	Sulfur

Monomer Name	Monomer Structure	SMILES	Number of Representations in Library	Represented Chemical Functionalities
4,4'-Dihydroxydiphenylmethane		Oc1ccc(cc1)Cc2ccc(cc2)O	6	Aromatic
4,4'-Isopropylidenedicyclohexanol, mixture of isomers		OC(CC1)CCC1C(C)(C)C(CC2)CCC2O	16	Ring
1,4-Dithiane-2,5-diol		OC(CS1)SCC1O	14	Sulfur
2,2-Diethyl-1,3-propanediol		OCC(CC)(CC)CO	15	
Bis(4-hydroxyphenyl) Sulfone		Oc1ccc(cc1)S(=O)(=O)c2ccc(cc2)O	8	Sulfur, Oxygen
Resorcinol		Oc1cccc(c1)O	10	Aromatic
Biphenyl-2,2'-diol		Oc(cccc1)c1c2c(cccc2)O	5	Aromatic
2-Butyne-1,4-diol		OCC#CCO	6	Triple Bond
3-methyl-1,5-pentanediol		OCCC(C)CCO	14	
2,5-dimethyl-3-hexyne-2,5-diol		OC(C)(C)C#CC(C)(C)O	2	Triple Bond
Tripropylene glycol		OC(C)COC(C)COC(C)CO	10	Oxygen

45

Monomer Name	Monomer Structure	SMILES	Number of Representations in Library	Represented Chemical Functionalities
1,3-Propanediol		OCCCO	16	
1,5-pentanediol		OCCCCCO	15	
Dipropylene Glycol		OCC(C)OCC(C)O	9	Oxygen
1,4-Butanediol		OCCCCO	15	
1,6-Hexanediol		OCCCCCCO	15	
2-Methyl-1,3-propanediol		OCC(C)CO	14	
2-Butyl-2-ethyl-1,3-propanediol		OCC(CC)(CCCC)CO	16	
1,5-hexadiene-3,5-diol		OC(C=C)C(C=C)O	1	Double Bond
Ethylene Glycol		OCCO	48	
1,2-Propanediol		OCC(C)O	20	
1,7-heptanediol		OCCCCCCCO	7	
1,4-Cyclohexanedimethanol		OCC(CC1)CCC1CO	13	Ring

Table S2: Details of Monomers Incompatible with Synthesis

Monomer Name	SMILES	Incompatibility Hypothesis
4,4'-Methylenebis(2,6-di-tert-butylphenol)	CC(C)(C)C1=CC(=CC(=C1O)C(C)(C)C)CC2=CC(=C(C(=C2)C(C)(C)C)O)C(C)(C)C	Sterically hindered Alcohol Groups
Pinacol	OC(C)(C)C(C)(C)O	Can undergo Pinacol Rearrangement, preventing chain growth
2,4,7,9-Tetramethyl-5-decyne-4,7-diol	OC(C)(CC(C)C)C#CC(C)(CC(C)C)O	Sterically hindered Alcohol Groups, stabilized oxygen anion
trans-p-menth-6-ene-2,8-diol	OC(C)(C)C(CC=C1(C))CC1O	Sterically hindered Alcohol Groups, stabilized oxygen anion
Phenol Red, Free Acid	Oc1ccc(cc1)C2(OS(=O)(=O)c3ccccc23)c4ccc(O)cc4	Resonance Structure involving alcohol groups
Malonic Acid	OC(=O)CC(=O)O	Decomposition, Instability at synthesis temperatures

Table S3: Synthetic Procedures

Label	Procedure
M1	To a 20mL vial with a Teflon stir bar, diol (1.05 equiv) and dicarboxylic acid (1 equiv) were added. The vial was then fitted with a septum cap and purged with nitrogen. The vial is heated to 150 °C for 1 hour under 1 atm of nitrogen, followed by heating to 175 °C for 1 hour before being placed under vacuum (~10 torr) and cooled to 150 °C for an additional 2 hours. Following that, the vial was refilled with nitrogen (1 atm) and titanium (IV) isopropoxide (0.02 equiv) was added. The reaction was allowed to stir for 30 min before being placed back under vacuum for 12 hours and increasing the temperature to 180 °C.
M2	To a 20mL vial with a Teflon stir bar, diol (1.01 to 1.1 equiv) and dicarboxylic acid (1 equiv) were added. The vial was then fitted with a septum cap and purged with nitrogen. The vial was heated to 180 °C for 1.5 hours under 1 atm of nitrogen. Titanium (IV) isopropoxide (0.02 equiv) was added, and the reaction was allowed to stir for 30 minutes. Vacuum (~25 torr) was introduced, and the reaction was heated to 200 °C for 1 hour. The reaction temperature was increased to 250 °C, and reacted overnight. The vial was refilled with nitrogen (1 atm), cooled to 200 °C, and additional titanium isopropoxide (0.02 equiv) was added and allowed to stir for 1 hour. Vacuum was reintroduced, and the temperature was increased to 350C for an additional 16 hours.
M3	To a 20mL vial with a Teflon stir bar, diol (1.0 to 1.1 equiv) and dicarboxylic acid (1 equiv) were added. The vial was then fitted with a septum cap and purged with nitrogen. The vial was heated in the following sequence: 120 °C for 45 minutes, 150 °C for 45 min, and then 170 °C for 20minutes under 1 atm of nitrogen. Vacuum (~10 torr) was applied for 30 minutes at 170 °C before nitrogen (1 atm) was reintroduced, titanium (IV) isopropoxide (0.02 equiv) was added, and the reaction was allowed to stir for 15 minutes. Vacuum (~10 torr) was introduced, and the reaction was heated to 200 °C overnight.
M4	To a 20mL vial with a Teflon stir bar, diol (1.0 to 1.1 equiv) and dicarboxylic acid (1 equiv) were added. The vial was then fitted with a septum cap and purged with nitrogen. The vial was heated in the following sequence: 130 °C for 30 minutes, 150 °C for 1 hour, and then 180 °C for 1.5 hourss under 1 atm of nitrogen. Vacuum (~10 torr) was applied for 1 hour at 180 °C before nitrogen (1 atm) was reintroduced, the vial was cooled to 150 °C, and titanium (IV) isopropoxide (0.02 equiv) was added. The reaction was allowed to stir for 15 minutes. Vacuum (~10 torr) was reintroduced, and the reaction was heated at 180 °C overnight.
M5	To a 20mL vial with a Teflon stir bar, diol (1.0 to 1.1 equiv) and dicarboxylic acid (1 equiv) were added. The vial was then fitted with a septum cap and purged with nitrogen. The vial was heated to 150 °C for 1 hour, and then 170 °C for 1 hour under 1 atm of nitrogen. Vacuum (~10 torr) was applied for 1.5 hours at 170 °C before nitrogen (1 atm) was reintroduced and titanium (IV) isopropoxide (0.02 equiv) was added. The reaction was allowed to stir for 15 minutes. Vacuum (~10 torr) was reintroduced, and the reaction was heated at 180 °C overnight.

Label	Procedure
M6	To a 20mL vial with a Teflon stir bar, diol (1.0 to 1.1 equiv) and dicarboxylic acid (1 equiv) were added. The vial was then fitted with a septum cap and purged with nitrogen. The vial was heated in the following sequence: 110 °C for 45 minutes, 150 °C for 45 min, and then 175 °C for 45minutes under 1 atm of nitrogen. Vacuum (~10 torr) was applied for 2 hours at 175 °C before nitrogen (1 atm) was reintroduced, titanium (IV) isopropoxide (0.02 equiv) was added, and the reaction was allowed to stir for 15 minutes. Vacuum (~10torr) was introduced, and the reaction was heated to 180 °C overnight.
M7	To a 20mL vial with a Teflon stir bar, diol (1.0 to 1.1 equiv) and dicarboxylic acid (1 equiv) were added. The vial was then fitted with a septum cap and purged with nitrogen. The vial was heated to 150 °C for 1 hour, followed by 180 °C for 1.5 hours under 1 atm of nitrogen. Titanium (IV) isopropoxide (0.02 equiv) was added, and the reaction was allowed to stir for 30 minutes. Vacuum (~10torr) was introduced, and the reaction was heated to 200 °C for 1 hour. The reaction temperature was increased to 220 °C, and reacted overnight.
M8	To a 20mL vial with a Teflon stir bar, diol (1.0 to 1.1 equiv) and dicarboxylic acid (1 equiv) were added. The vial was then fitted with a septum cap and purged with nitrogen. The vial was heated in the following sequence: 120 °C for 1.5 hours, 150 °C for 1 hour, and then 180 °C for 45minutes under 1 atm of nitrogen. Titanium (IV) isopropoxide (0.02 equiv) was added, and the reaction was allowed to stir for 30 minutes. Vacuum (~10torr) was introduced, and the reaction was heated to 180 °C overnight.
M9	To a 20mL vial with a Teflon stir bar, diol (1.0 to 1.1 equiv) and dicarboxylic acid (1 equiv) were added. The vial was then fitted with a septum cap and purged with nitrogen. The vial was heated in the following sequence: 120 °C for 45 minutes, 150 °C for 45 min, and then 180 °C for 45minutes under 1 atm of nitrogen. Vacuum (~10 torr) was applied for 30 minutes at 180 °C before nitrogen (1 atm) was reintroduced, titanium (IV) isopropoxide (0.02 equiv) was added, and the reaction was allowed to stir for 30 minutes. Vacuum (~10torr) was introduced, and the reaction was heated to 180 °C overnight.
M10	To a 20mL vial with a Teflon stir bar, diol (1.0 to 1.1 equiv) and dicarboxylic acid (1 equiv) were added. The vial was then fitted with a septum cap and purged with nitrogen. The vial was heated in the following sequence: 140 °C for 1 hour, 165 °C for 1 hour, and then 180 °C for 45minutes under 1 atm of nitrogen. Vacuum (~10 torr) was applied for 45 minutes at 180 °C before nitrogen (1 atm) was reintroduced, titanium (IV) isopropoxide (0.02 equiv) was added, and the reaction was allowed to stir for 30 minutes. Vacuum (~10torr) was introduced, and the reaction was heated to 180 °C overnight.
M11	To a 20mL vial with a Teflon stir bar, diol (1.0 to 1.1 equiv) and dicarboxylic acid (1 equiv) were added. The vial was then fitted with a septum cap and purged with nitrogen. The vial was heated in the following sequence: 105 °C for 1.5 hours, 170 °C for 1.5 hours, and then 190 °C for 45minutes under 1 atm of nitrogen. Titanium (IV) isopropoxide (0.02 equiv) was added, and the reaction was allowed to stir for 30 minutes. Vacuum (~10torr) was introduced, and the reaction was heated to 190 °C overnight.

Label	Procedure
M12	To a 20mL vial with a Teflon stir bar, diol (1.0 to 1.1 equiv) and dicarboxylic acid (1 equiv) were added. The vial was then fitted with a septum cap and purged with nitrogen. The vial was heated to 140 °C for 2 hours, followed by 180 °C for 1.5 hours under 1 atm of nitrogen. Titanium (IV) isopropoxide (0.02 equiv) was added, and the reaction was allowed to stir for 30 minutes. Vacuum (~10torr) was introduced, and the reaction was heated to 180 °C overnight.
M13	To a 20mL vial with a Teflon stir bar, diol (1.0 to 1.1 equiv) and dicarboxylic acid (1 equiv) were added. The vial was then fitted with a septum cap and purged with nitrogen. The vial was heated in the following sequence: 140 °C for 1.5 hours, 160 °C for 1 hour, and then 180 °C for 45minutes under 1 atm of nitrogen. Titanium (IV) isopropoxide (0.02 equiv) was added, and the reaction was allowed to stir for 30 minutes. Vacuum (~10torr) was introduced, and the reaction was heated to 180 °C overnight.
M14	To a 20mL vial with a Teflon stir bar, diol (1.0 to 1.1 equiv) and dicarboxylic acid (1 equiv) were added. The vial was then fitted with a septum cap and purged with nitrogen. The vial was heated in the following sequence: 110 °C for 30 minutes, 120 °C for 1 hour, 150 °C for 1 hour, and finally 180 °C for 45minutes under 1 atm of nitrogen. Titanium (IV) isopropoxide (0.02 equiv) was added, and the reaction was allowed to stir for 30 minutes. Vacuum (~10torr) was introduced, and the reaction was heated to 180 °C overnight.
M15	To a 20mL vial with a Teflon stir bar, diol (1.0 to 1.1 equiv) and dicarboxylic acid (1 equiv) were added. The vial was then fitted with a septum cap and purged with nitrogen. The vial was heated in the following sequence: 120 °C for 1 hour, 140 °C for 1 hour, 160 °C for 45 minutes and finally 180 °C for 45 minutes under 1 atm of nitrogen. Titanium (IV) isopropoxide (0.02 equiv) was added, and the reaction was allowed to stir for 30 minutes. Vacuum (~10torr) was introduced, and the reaction was heated to 180 °C overnight.
M16	To a 20mL vial with a Teflon stir bar, diol (1.0 to 1.1 equiv) and dicarboxylic acid (1 equiv) were added. The vial was then fitted with a septum cap and purged with nitrogen. The vial was heated in the following sequence: 120 °C for 1.5 hour, 150 °C for 1.5 hours, and finally 170 °C for 45 minutes under 1 atm of nitrogen. Titanium (IV) isopropoxide (0.02 equiv) was added, and the reaction was allowed to stir for 30 minutes. Vacuum (~10torr) was introduced, and the reaction was heated to 170 °C overnight.
M17	To a 20mL vial with a Teflon stir bar, diol (1.0 to 1.1 equiv) and dicarboxylic acid (1 equiv) were added. The vial was then fitted with a septum cap and purged with nitrogen. The vial was heated in the following sequence: 130 °C for 2 hours, 150 °C for 1.5 hours, and finally 170 °C for 45 minutes under 1 atm of nitrogen. Titanium (IV) isopropoxide (0.02 equiv) was added, and the reaction was allowed to stir for 30 minutes. Vacuum (~10torr) was introduced, and the reaction was heated to 170 °C overnight.
M18	To a 20mL vial with a Teflon stir bar, diol (1.0 to 1.1 equiv) and dicarboxylic acid (1 equiv) were added. The vial was then fitted with a septum cap and purged with nitrogen. The vial was heated to 110 °C for 1.5 hours, followed by 140 °C for 1 hour under 1 atm of nitrogen. Vacuum (~10 torr) was applied for 1 hour at 150 °C before nitrogen (1 atm) was reintroduced, and titanium (IV) isopropoxide (0.02 equiv) was added. The reaction was allowed to stir for 15 minutes. Vacuum (~10torr) was reintroduced, and the reaction was heated at 170 °C overnight.

Label	Procedure
M19	To a 20mL vial with a Teflon stir bar, diol (1.0 to 1.1 equiv) and dicarboxylic acid (1 equiv) were added. The vial was then fitted with a septum cap and purged with nitrogen. The vial was heated to 110 °C for 2 hours, followed by 140 °C for 1 hour, and 150 °C for 4 hours under 1 atm of nitrogen. Vacuum (~10 torr) was applied for 1.5 hours at 150 °C before nitrogen (1 atm) was reintroduced, and titanium (IV) isopropoxide (0.02 equiv) was added. The reaction was allowed to stir for 30 minutes. Vacuum (~10torr) was reintroduced, and the reaction was heated at 180 °C overnight.
M20	To a 20mL vial with a Teflon stir bar, diol (1.0 to 1.1 equiv) and dicarboxylic acid (1 equiv) were added. The vial was then fitted with a septum cap and purged with nitrogen. The vial was heated to 110 °C for 1 hour2, followed by 140 °C for 1 hour, and 160 °C for 1 hour under 1 atm of nitrogen. Vacuum (~10 torr) was applied for 1.5 hours at 160 °C before nitrogen (1 atm) was reintroduced, and titanium (IV) isopropoxide (0.02 equiv) was added. The reaction was allowed to stir for 30 minutes. Vacuum (~10torr) was reintroduced, and the reaction was heated at 170 °C overnight.
M21	To a 20mL vial with a Teflon stir bar, diol (1.0 to 1.1 equiv) and dicarboxylic acid (1 equiv) were added. The vial was then fitted with a septum cap and purged with nitrogen. The vial was heated to 120 °C for 2.5 hours, followed by 150 °C for 1 hour, and 160 °C for 1 hour under 1 atm of nitrogen. Vacuum (~10 torr) was applied for 2 hours at 160 °C before nitrogen (1 atm) was reintroduced, and titanium (IV) isopropoxide (0.02 equiv) was added. The reaction was allowed to stir for 30 minutes. Vacuum (~10torr) was reintroduced, and the reaction was heated at 170 °C overnight.
M22	To a 20mL vial with a Teflon stir bar, diol (1.0 to 1.1 equiv) and dicarboxylic acid (1 equiv) were added. The vial was then fitted with a septum cap and purged with nitrogen. The vial was heated in the following sequence: 110 °C for 1 hour, 120 °C for 1 hour, 150 °C for 3 hours, and then 180 °C for 45minutes under 1 atm of nitrogen. Vacuum (~10 torr) was applied for 2 hours at 180 °C before nitrogen (1 atm) was reintroduced, and titanium (IV) isopropoxide (0.02 equiv) was added. The reaction was allowed to stir for 30 minutes. Vacuum (~10torr) was reintroduced, and the reaction was heated at 180 °C overnight.
M23	To a 20mL vial with a Teflon stir bar, diol (1.0 to 1.1 equiv) and dicarboxylic acid (1 equiv) were added. The vial was then fitted with a septum cap and purged with nitrogen. The vial was heated to 150 °C for 1 hour2, followed by 180 °C for 1 hour, and 195 °C for 1 hour under 1 atm of nitrogen. Vacuum (~10 torr) was applied for 1.5 hours at 195 °C before nitrogen (1 atm) was reintroduced, and titanium (IV) isopropoxide (0.02 equiv) was added. The reaction was allowed to stir for 30 minutes. Vacuum (~10torr) was reintroduced, and the reaction was heated at 195 °C overnight.
M24	To a vial with a Teflon stir bar, diol (1 to 1.2 equiv), dicarboxylic acid methyl ester (1 equiv), Titanium (IV) Isopropoxide (0.02 equiv), and titanium (IV) butoxide (0.02 equiv) were added. The vial is then fitted with a septum cap and purged with nitrogen. The vial is heated in the following sequence: 110 °C for 1 hour, 120 °C for 1.5 hours, 155 °C for 2 hours, and 170 °C for 30 minutes under 1 atm of nitrogen. Vacuum (~10torr) is then applied while heating to 170 °C overnight.

Label	Procedure
M25	To a vial with a Teflon stir bar, diol (1 to 1.2 equiv) and dicarboxylic acid (1 equiv) were added. The vial is then fitted with a septum cap and purged with nitrogen. The vial is heated to 160 °C for 2 hours under 1 atm of nitrogen, before being placed under vacuum (~10 torr) for an additional 2 hours. Following that, the vial was refilled with nitrogen (1 atm) and titanium (IV) isopropoxide (0.001 equiv) was added. The reaction was allowed to stir for 30 min before being placed back under vacuum for 12 hours and increasing the temperature to 180 °C.
M26	Monomer and catalyst were added to a vial with a stir bar. The vial was sealed and warmed to 150 °C for 4 hours under nitrogen gas flow. The temperature was raised to 180 °C and vacuum (50 mmHg) was applied overnight. The reaction was considered complete after the reaction mixture was solidified. The polymer product was used without furthur purification
M27	To a 20mL vial with a Teflon stir bar, diol (1 equiv), dimethyl carbonate (2 equiv), and DMAP (0.01 equiv) were added. The vial was then fitted with a septum cap and purged with nitrogen. The vial was heated to 75 °C for 3 hours, followed by 95 °C for 2 hours under 1 atm of nitrogen. The vial was then placed under vacuum (~10 torr) and heated to 1o5 °C overnight.
M28	To a 20mL vial with a Teflon stir bar, diol (1 equiv), dimethyl carbonate (2 equiv), and DMAP (0.01 equiv) were added. The vial was then fitted with a septum cap and purged with nitrogen. The vial was heated in the following sequence: 75 °C for 1 hour, 90 °C for 1 hour, and then 115 °C for 1 hours under 1 atm of nitrogen. The vial was then placed under vacuum (~10 torr) and heated to 130 °C overnight.
M29	To a 20mL vial with a Teflon stir bar, diol (1 equiv), dimethyl carbonate (2 equiv), and DMAP (0.01 equiv) were added. The vial was then fitted with a septum cap and purged with nitrogen. The vial was heated in the following sequence: 70 °C for 3.5 hours, 90 °C for 1.5 hours, and then 130 °C for 1 hour under 1 atm of nitrogen. The vial was then placed under vacuum (~10 torr) and heated to 130 °C overnight.
M30	To a 20mL vial with a Teflon stir bar, diol (1 equiv), dimethyl carbonate (2 equiv), and DMAP (0.01 equiv) were added. The vial was then fitted with a septum cap and purged with nitrogen. The vial was heated in the following sequence: 75 °C for 2.5 hours, 90 °C for 1 hour, and then 115 °C for 2 hours under 1 atm of nitrogen. The vial was then placed under vacuum (~10 torr) and at 115 °C for 1 hour before being heated to 150 °C overnight under vacuum.
M31	A vial with a septum cap and Teflon stir bar was prepared for the reaction by drying it in an oven overnight, then purged with nitrogen and then chilled (0 °C). Diol (1 equiv), diacid chloride (1 equiv), TCE (1 M) then were added to the vial. The reaction was initiated with a the slow addition (over 10 min) of pyridine(8 equiv) resulting in solid formation. After 10 min, the water bath was removed, and stirred overnight. The resulting mixture was poured into methanol. The precipitated polymer was collected with vacuum filtration and dried in vacuo to give a solid.
M32	In a 20mL vial, diol (1 equiv) was dissolved in solvent (water or DMF, 7.5mL) with base (1.3 equiv) and a SpinPlus stir bar was added. In a second 20mL vial, acid chloride (1.1mL) was added to a second solvent immiscible with the first (Diethyl Ether, Diisopropyl Ether, Hexanes, or Cyclohexane, 7.5mL). After dissolution of the acid chloride, the solution was added dropwise to the stirring (600 rpm) diol solution. The resulting interfacial reaction was left stirring overnight, and the resulting polymer was precipitated into methanol (200mL).

Label	Procedure
M33	In a nitrogen atmosphere glovebox, the following steps were performed. To a 20mL vial with a Teflon stir bar, THF (6.5 mL), monomer (1000 equiv) and TBD catalyst (5 equiv) were added and mixed. Subsequently, benzyl alcohol (initiator, 20 equiv) was added, and the reaction was capped and stirred for 20 hours. The reaction was uncapped, and benzoic acid (40 equiv) was added as a quenching agent and subsequently removed from the glovebox.
M34	In a nitrogen atmosphere glovebox, monomer(s) (1000 equiv, optionally 500 equiv of second monomer) and TBD catalyst (5 equiv) were added to a 20mL vial with a Teflon stir bar and mixed. Subsequently, benzyl alcohol (initiator, 20 equiv) was added. The vial was capped and sealed, and removed from the glovebox. While sealed, the vial was heated to 120 °C for 20hours.
M35	To a 20mL vial with a Teflon Stir bar, monomer (1000 equiv) and triphephenyl bismuth (30 equiv) were added. The reaction was stirred at 110 °C for 20 hours.
M36	To a 20mL vial with a Teflon Stir bar, monomers (1000 equiv, 500 equiv), triphephenyl bismuth (30 equiv), and tin octoate (10 equiv) were added. The reaction was stirred at 110 °C for 20 hours.

Table Table S4: Unsuccessful Reactions

Number	Monomer 1	Monomer 2	Method
1	Malonyl Chloride	cis-2-Butene-1,4-diol	M32
2	Terephthaloyl Chloride	2,2-diethyl-1,3-propanediol	M32
3	Terephthaloyl Chloride	1,2-propanediol	M32
4	Malonyl Chloride	Tripropylene glycol	M32
5	Malonyl Chloride	Resorcinol	M32
6	Phthaloyl Chloride	1,3-Bis[2-(4-hydroxyphenyl)-2-propyl]benzene	M32
7	Phthaloyl Chloride	4,4'-(alpha-Methylbenzylidene)bisphenol	M32
8	Phthaloyl Chloride	4,4'-Isopropylidenedicyclohexanol, mixture of isomers	M32
9	Phthaloyl Chloride	4,4'-(9-Fluorenylidene)diphenol	M32
10	Phthaloyl Chloride	4,4'-Cyclohexylidenebisphenol	M32
11	Phthaloyl Chloride	(R)-(+)-1,1'-Binaphthyl-2,2'-diol	M32
12	Phthaloyl Chloride	2,2'-Thiodiethanol	M32
13	Phthaloyl Chloride	Biphenyl-2,2'-diol	M32
14	Phthaloyl Chloride	1,3-Propanediol	M32
15	Phthaloyl Chloride	1,5-pentanediol	M32
16	Phthaloyl Chloride	1,8-octanediol	M32
17	Phthaloyl Chloride	1,9-nonanediol	M32
18	Malonyl Chloride	2,7-Naphthalenediol	M32
19	Phthaloyl Chloride	1,10-decanediol	M32
20	Phthaloyl Chloride	2,2-diethyl-1,3-propanediol	M32
21	Phthaloyl Chloride	2,2-Dimethyl-1,3-propanediol	M32
22	Phthaloyl Chloride	4,8-Bis(hydroxymethyl)tricyclo[5.2.1.02,6]decane	M32
23	Phthaloyl Chloride	1,2-propanediol	M32
24	Phthaloyl Chloride	2,3-Butanediol	M32
25	Phthaloyl Chloride	1,4-cyclohexanediol	M32
26	Phthaloyl Chloride	diethylene glycol	M32
27	Phthaloyl Chloride	triethylene glycol	M32
28	Malonyl Chloride	2-Butyne-1,4-diol	M32
29	Diglycolyl Chloride	Bis(4-hydroxyphenyl) Sulfone	M32
30	Phthaloyl Chloride	dipropylene glycol	M32
31	Phthaloyl Chloride	Tripropylene glycol	M32
32	Phthaloyl Chloride	Resorcinol	M32
33	Diglycolyl Chloride	4,4'-Isopropylidenebis(2,6-dimethylphenol)	M32
34	Phthaloyl Chloride	2-Butyne-1,4-diol	M32
35	Phthaloyl Chloride	ethylene glycol	M32
36	Phthaloyl Chloride	1,4-Butanediol	M32
37	Phthaloyl Chloride	1,6-Hexanediol	M32
38	Phthaloyl Chloride	2-Methyl-1,3-propanediol	M32
39	Phthaloyl Chloride	2-Butyl-2-ethyl-1,3-propanediol	M32
40	Diglycolyl Chloride	Dipropylene Glycol	M32
41	Diglycolyl Chloride	Biphenyl-2,2'-diol	M32
42	Diglycolyl Chloride	2-Butyne-1,4-diol	M32
43	diglycolyl chloride	2,5-dimethyl-3-hexyne-2,5-diol	M32
44	diglycolyl chloride	trans-p-menth-6-ene-2,8diol	M32
45	Sebacoyl Chloride	Phenol Red	M32

46	Oxalyl Chloride	4,4′-(9-Fluorenylidene)diphenol	M32
47	Oxalyl Chloride	4,4′-Cyclohexylidenebisphenol	M32
48	Oxalyl Chloride	(R)-(+)-1,1′-Binaphthyl-2,2′-diol	M32
49	Oxalyl Chloride	4,4′-Thiodiphenol	M32
50	Oxalyl Chloride	Guaiacol glyceryl ether	M32
51	Oxalyl Chloride	2,2′-Thiodiethanol	M32
52	Oxalyl Chloride	Dianhydro-D-glucitol	M32
53	Oxalyl Chloride	cis-2-Butene-1,4-diol	M32
54	Oxalyl Chloride	Biphenyl-2,2′-diol	M32
55	Oxalyl Chloride	1,3-Propanediol	M32
56	Oxalyl Chloride	1,5-pentanediol	M32
57	Oxalyl Chloride	1,9-nonanediol	M32
58	Oxalyl Chloride	2,2-Dimethyl-1,3-propanediol	M32
59	Oxalyl Chloride	1,2-propanediol	M32
60	Oxalyl Chloride	2,3-Butanediol	M32
61	Oxalyl Chloride	1,4-cyclohexanediol	M32
62	Oxalyl Chloride	diethylene glycol	M32
63	Oxalyl Chloride	triethylene glycol	M32
64	Oxalyl Chloride	4,4′-Sulfonylbis(2-methylphenol)	M32
65	Oxalyl Chloride	2-Hydroxyethyl disulfide	M32
66	Oxalyl Chloride	dipropylene glycol	M32
67	Oxalyl Chloride	Tripropylene glycol	M32
68	Oxalyl Chloride	Resorcinol	M32
69	Oxalyl Chloride	Naphthalene-1,5-diol	M32
70	Oxalyl Chloride	2-Butyne-1,4-diol	M32
71	Oxalyl Chloride	Bisphenol A	M32
72	Oxalyl Chloride	Bis(4-hydroxyphenyl) Sulfone	M32
73	Oxalyl Chloride	ethylene glycol	M32
74	Oxalyl Chloride	1,4-Butanediol	M32
75	Oxalyl Chloride	1,6-Hexanediol	M32
76	Oxalyl Chloride	2-Methyl-1,3-propanediol	M32
77	Oxalyl Chloride	2-Butyl-2-ethyl-1,3-propanediol	M32
78	Oxalyl Chloride	3-methyl-1,5-pentanediol	M32
79	Succinyl Chloride	1,3-Bis[2-(4-hydroxyphenyl)-2-propyl]benzene	M32
80	Succinyl Chloride	Diethylene Glycol	M32
81	Succinyl Chloride	Triethylene Glycol	M32
82	Isophthaloyl Chloride	4,4′-Isopropylidenedicyclohexanol, mixture of isomers	M32
83	Isophthaloyl Chloride	2,2-Diethyl-1,3-propanediol	M32
84	Isophthaloyl Chloride	4,4′-Dihydroxydiphenylmethane	M32
85	Isophthaloyl Chloride	4,4′-(9-Fluorenylidene)diphenol	M32
86	Isophthaloyl Chloride	Triethylene Glycol	M32
87	Isophthaloyl Chloride	Dipropylene Glycol	M32
88	Isophthaloyl Chloride	Tripropylene glycol	M32
89	Isophthaloyl Chloride	Guaiacol glyceryl ether	M32
90	Isophthaloyl Chloride	Biphenyl-2,2′-diol	M32
91	Isophthaloyl Chloride	2-Butyne-1,4-diol	M32
92	Isophthaloyl Chloride	2-Hydroxyethyl disulfide	M32
93	Oxalyl chloride	1,5-hexadiene-3,5-diol	M32

94	Oxalyl chloride	trans-p-menth-6-ene-2,8diol	M32
95	Oxalyl chloride	2,4,7,9-Tetramethyl-5-decyne-4,7-diol	M32
96	Oxalyl chloride	2,5-dimethyl-3-hexyne-2,5-diol	M32
98	Succinyl Chloride	trans-p-menth-6-ene-2,8diol	M32
99	Succinyl Chloride	2,4,7,9-Tetramethyl-5-decyne-4,7-diol	M32
100	Succinyl Chloride	2,5-dimethyl-3-hexyne-2,5-diol	M32
101	Adipoyl Chloride	Dianhydro-D-glucitol	M32
102	adipoyl chloride	trans-p-menth-6-ene-2,8diol	M32
103	Azelaoyl Chloride	1,5-hexadiene-3,5-diol	M32
104	adipoyl chloride	1,5-hexadiene-3,5-diol	M32
105	Sebacoyl Chloride	1,5-hexadiene-3,5-diol	M32
106	terephthaloyl chloride	1,5-hexadiene-3,5-diol	M32
107	Isophthaloyl Chloride	trans-p-menth-6-ene-2,8diol	M32
108	terephthaloyl chloride	trans-p-menth-6-ene-2,8diol	M32
109	Malonyl Chloride	trans-p-menth-6-ene-2,8diol	M32
110	Azelaoyl Chloride	trans-p-menth-6-ene-2,8diol	M32
111	Sebacoyl Chloride	trans-p-menth-6-ene-2,8diol	M32
112	terephthaloyl chloride	2,5-dimethyl-3-hexyne-2,5-diol	M32
113	Sebacoyl Chloride	4,4′-Isopropylidenedicyclohexanol, mixture of isomers	M32
114	Azelaoyl Chloride	2,5-dimethyl-3-hexyne-2,5-diol	M32
115	Malonyl Chloride	2,5-dimethyl-3-hexyne-2,5-diol	M32
116	adipoyl chloride	2,5-dimethyl-3-hexyne-2,5-diol	M32
117	Malonyl Chloride	1,5-hexadiene-3,5-diol	M32
118	Succinyl Chloride	2,4,7,9-Tetramethyl-5-decyne-4,7-diol	M32
119	Sebacoyl Chloride	2,4,7,9-Tetramethyl-5-decyne-4,7-diol	M32
120	terephthaloyl chloride	2,4,7,9-Tetramethyl-5-decyne-4,7-diol	M32
121	Isophthaloyl Chloride	2,4,7,9-Tetramethyl-5-decyne-4,7-diol	M32
122	adipoyl chloride	2,4,7,9-Tetramethyl-5-decyne-4,7-diol	M32
123	Suberoyl chloride	2,4,7,9-Tetramethyl-5-decyne-4,7-diol	M32
124	Sebacoyl Chloride	Pinacol	M32
125	Sebacoyl Chloride	4,4'-Methylenebis(2,6-di-tert-butylphenol)	M32
126	Malonyl Chloride	4,4-Thiodiphenol	M32
127	Terephthaloyl Chloride	Phenol Red	M32
128	Sebacoyl Chloride	Biphenyl-2,2′-diol	M32
129	Azelaoyl chloride	2,2′-Thiodiethanol	M32
130	Malonyl Chloride	Guaiacol glyceryl ether	M32
131	Azelaoyl chloride	Dianhydro-D-glucitol	M32
132	Azelaoyl chloride	4,4′-Sulfonylbis(2-methylphenol)	M32
133	Malonyl Chloride	2,2′-Thiodiethanol	M32
134	Azelaoyl chloride	4,4'-Methylenebis(2,6-di-tert-butylphenol)	M32
135	Azelaoyl chloride	4,4′-Cyclohexylidenebisphenol	M32
136	Suberoyl chloride	2,2′-Thiodiethanol	M32
137	Suberoyl chloride	cis-2-Butene-1,4-diol	M32
138	Malonyl Chloride	Dianhydro-D-glucitol	M32
139	Dimethylmalonyl chloride	2,2′-Thiodiethanol	M32
140	Dimethylcarbonate	1,4-dithiane-2,5-diol	M28
141	Dimethylcarbonate	Dianhydro-D-glucitol	M27
142	Dimethylcarbonate	Biphenyl-2,2′-diol	M27

143	Dimethylcarbonate	2,5-hexanediol(+isomers)	M28
144	Dimethylcarbonate	1,2-propanediol	M27
145	Dimethylcarbonate	2,3-Butanediol	M27
146	Dimethylcarbonate	triethylene glycol	M27
147	Dimethylcarbonate	Tripropylene glycol	M29
148	Dimethylcarbonate	Resorcinol	M28
149	Dimethylcarbonate	ethylene glycol	M29
150	Dimethylcarbonate	3-methyl-1,5-pentanediol	M30
151	Dimethylcarbonate	2,2,4-Trimethyl-1,3-pentanediol	M30
152	dimethylcarbonate	trans-p-menth-6-ene-2,8diol	M30
153	dimethylcarbonate	2,5-dimethyl-3-hexyne-2,5-diol	M30
154	[(Carboxymethyl)(methyl)amino]acetic acid	ethylene glycol	M25
155	[(Carboxymethyl)(methyl)amino]acetic acid	1,3-Propanediol	M25
156	adipic acid	Dianhydro-D-glucitol	M25
157	succinic acid	pinacol	M25
158	adipic acid	cis-2-Butene-1,4-diol	M25
159	succinic acid	1,2-propanediol	M25
160	Malonic Acid	ethylene glycol	M25
161	Malonic Acid	1,9-nonanediol	M25
162	Malonic Acid	1,10-decanediol	M25
163	Malonic Acid	1,3-Propanediol	M25
164	Malonic Acid	1,4-Butanediol	M25
165	Malonic Acid	1,5-pentanediol	M25
166	Malonic Acid	1,6-hexanediol	M25
167	Malonic Acid	2,5-hexanediol(+isomers)	M25
168	Malonic Acid	3-methyl-1,5-pentanediol	M25
169	Malonic Acid	1,7-heptanediol	M25
170	Malonic Acid	1,8-octanediol	M25
171	[(Carboxymethyl)(methyl)amino]acetic acid	1,9-nonanediol	M12
172	2,6-Naphthalenedicarboxylic Acid	1,10-decanediol	M12
173	[(Carboxymethyl)(methyl)amino]acetic acid	diethylene glycol	M13
174	2,2′-[ethylenebis(oxy)] bisacetic acid	diethylene glycol	M20
175	Diglycolic acid	diethylene glycol	M20
176	succinic acid	diethylene glycol	M20
177	pimelic acid	triethylene glycol	M14
178	glutaric acid	triethylene glycol	M20
179	2,2′-[ethylenebis(oxy)] bisacetic acid	triethylene glycol	M20
180	Diglycolic acid	triethylene glycol	M20
181	isophthalic acid	triethylene glycol	M20
182	succinic acid	triethylene glycol	M20
183	2,6-Naphthalenedicarboxylic Acid	Tripropylene glycol	M15
184	2,2′-[ethylenebis(oxy)] bisacetic acid	2-methyl-1,3-propanediol	M18
185	2,2′-[ethylenebis(oxy)] bisacetic acid	Tripropylene glycol	M21
186	diglycolic acid	Tripropylene glycol	M21
187	isophthalic acid	Tripropylene glycol	M21
188	adipic acid	Tripropylene glycol	M21

189, 190a	[(Carboxymethyl)(methyl)amino]acetic acid	2-methyl-1,3-propanediol	M18
190b	2,2′-[ethylenebis(oxy)] bisacetic acid	dipropylene glycol	M21
191	isophthalic acid	dipropylene glycol	M21
192	2,6-Naphthalenedicarboxylic Acid	2-methyl-1,3-propanediol	M18
193	Succinic acid	dipropylene glycol	M15
194	isophthalic acid	Guaiacol glyceryl ether	M16
195	Sebacic Acid	1,4-dithiane-2,5-diol	M21
196	quinoline-2,4-dicarboxylic acid	diethylene glycol	M23
197	adipic acid	Dianhydro-D-glucitol	M21
198	isophthalic acid	2-methyl-1,3-propanediol	M2
199	2,6-Naphthalenedicarboxylic Acid	3-methyl-1,5-pentanediol	M18
200	2,6-Naphthalenedicarboxylic Acid	1,4-cyclohexanediol	M5
201	2,6-Naphthalenedicarboxylic Acid	2,2-Diethyl-1,3-propanediol	M18
202	glutaric acid	2,3-Butanediol	M5
203	2,5-Furandicarboxylic Acid	ethylene glycol	M6
204	2,5-Furandicarboxylic Acid	2,3-Butanediol	M6
205	2,5-Furandicarboxylic Acid	1,6-hexanediol	M6
206	2,2′-[ethylenebis(oxy)] bisacetic acid	2,3-Butanediol	M6
207	2,6-Naphthalenedicarboxylic Acid	2,2-Dimethyl-1,3-propanediol	M7
208	pimelic acid	2,3-Butanediol	M9
209	2,6-Naphthalenedicarboxylic Acid	2,3-Butanediol	M19
210	isophthalic acid	4,4′-Isopropylidenedicyclohexanol, mixture of isomers	M2
211	2,2′-[ethylenebis(oxy)] bisacetic acid	ethylene glycol	M10
212	2,2′-[ethylenebis(oxy)] bisacetic acid	1,2-propanediol	M18
213	[(Carboxymethyl)(methyl)amino]acetic acid	1,2-propanediol	M19
214	lactide	e-caprolactone	M33
215	e-Decalactone	Massoia Lactone	M36
216	e-caprolactone	Massoia Lactone	M36
217	Undecanoic delta-lactone	Massoia Lactone	M36
218	delta-Nonalactone	Massoia Lactone	M36
219	pentadecanolide	Massoia Lactone	M36
220	B-butryolactone	Massoia Lactone	M36
221	5-Dodecanolide	Massoia Lactone	M36
222	16-hexadecanolide	Massoia Lactone	M36
223	Massoia Lactone	Undecanoic delta-lactone	M36
224	Massoia Lactone	Delta-nonalactone	M36
225	Massoia Lactone	B-Butyrolactone	M36
226	Massoia Lactone	5-Dodecanolide	M36
227	delta-Valerolactone	Massoia Lactone	M36
228	Undecanoic delta-lactone		M33
229	Undecanoic delta-lactone		M35
230	delta-Nonalactone		M33
231	delta-Nonalactone		M35
232	Massoia Lactone		M35
233	e-Decalactone	lactide	M36
234	Massoia Lactone	lactide	M36
235	Lactide		M33

236	lactide	coumarin	M36
237	coumarin	Massoia Lactone	M36
238	coumarin	Undecanoic delta-lactone	M36
239	coumarin	Delta-nonalactone	M36
240	coumarin	5-Dodecanolide	M36
241	Phthaloyl Chloride	Guaiacol glyceryl ether	M32
242	B-butryolactone	lactide	M36

Table S5: Biodegradation test results of commercial polymers.

Polymer	BigSMILES	Mn	Colony growth	Degradation behavior
P3HB	{[][<]C(=O)CC(C)O[>][]}	10 kDa	Yes	Classic clear zone
PBA	{[][<]C(=O)CCCCC(=O)OCCCCO[>], [<]C(=O)c(cc1)ccc1C(=O)OCCCCO[>][]}	12 kDa	Yes	Classic clear zone
PBAT	{[][<]C(=O)CC(C)O[>][]}	Unknown	Yes	Distributed degradation
PCL	{[][<]C(=O)CCCCCO[>][]}	80 kDa	Yes	No degradation
PCL diol	{[][<]OCCCCCC(=O)[>][]}OCCOCCO {[][<]C(=O)CCCCCO[>][]}	2 kDa	Yes	Classic clear zone
PLA	{[][<]C(=O)C(C)O[>][]}	20 kDa	Yes	No degradation

Table S6: Samples with no colony growth during clear zone test incubation.

1	111	199	566
5	113	200	568
16	116	216	576
35	124	217	583
41	125	233	597
46	128	248	600
51	130	251	601
52	137	254	603
55	145	270	605
58	153	347	606
61	154	462	609
63	158	465	617
73	161	466	619
75	163	471	630
77	169	473	638
80	170	475	639
82	175	476	640
85	182	477	641
91	185	480	642
94	186	497	643
100	187	520	644
101	188	532	651

102	189	535	589
103	191	556	
111	196	559	

Table S7: The substituted and unsubstituted compared chemistries for the study of the effect of heteroatoms on biodegradability.

Chemistry	Substituted monomer	Unsubstituted monomer
S	C(=O)CSCC(=O)	C(=O)CCCC(=O)
	OCCSCCO	OCCCCCO
	Oc1ccc(cc1)Sc2ccc(cc2)O	Oc1ccc(cc1)Cc2ccc(cc2)O
	OC(CS1)SCC1O	OC(CC1)CCC1O
S$_2$	OCCSSCCO	OCCCCCCO
SO$_2$	Oc1ccc(cc1)S(=O)(=O)c2ccc(cc2)O	Oc1ccc(cc1)Cc2ccc(cc2)O
	Oc1c(C)cc(cc1)S(=O)(=O)c2ccc(c(C)c2)O	Oc1c(C)cc(cc1)Cc2ccc(c(C)c2)O
N	C(=O)CN(C)CC(=O)	C(=O)CCCC(=O)
O	C(=O)COCC(=O)	C(=O)CCCC(=O)
	C(=O)COCCOCC(=O)	C(=O)CCCCCC(=O)
	OCCOCCO	OCCCCCO
	OCCOCCOCCO	OCCCCCCCCO
	OC(C)COC(C)COC(C)CO	OC(C)CCC(C)CCC(C)CO
C=C	OCC=CCO	OCCCCO
	C(=O)C=CCC(CCCCC)O	C(=O)CCCC(CCCCC)O
	C(=O)C=Cc(cccc1)c1O	C(=O)CCc(cccc1)c1O
C#C	OCC#CCO	OCCCCO
	OC(C)(C)C#CC(C)(C)O	OC(C)(C)CCC(C)(C)O

Table S8: Samples with no colony growth during clear zone test incubation. The BigSMILES indicated with a (*) has a 2:1 monomer ratio, therefore the 8 repeat ring is adapted to take into account this ratio. Other polymers have a 1:1 monomer ratio.

BigSMILES	8 repeat ring
{[][<]C(=O)CCC(=O)[<], [>]Oc1cccc(c1)O[>][]}	C1(=O)CCC(=O)Oc%(2)cccc(c%(2))OC(=O)CCC(=O)Oc%(3)cccc(c%(3))OC(=O)CCC (=O)Oc%(4)cccc(c%(4))OC(=O)CCC(=O)Oc%(5)cccc(c%(5))OC(=O)CCC(=O)Oc%(6) cccc(c%(6))OC(=O)CCC(=O)Oc%(7)cccc(c%(7))OC(=O)CCC(=O)Oc%(8)cccc(c%(8)) OC(=O)CCC(=O)Oc%(9)cccc(c%(9))O1
{[][<]C(=O)CCCC(=O)[<], [>]OCCO[>][]}	C1(=O)CCCC(=O)OCCOC(=O)CCCC(=O)OCCOC(=O)CCCC(=O)OCCOC(=O)CCCC (=O)OCCOC(=O)CCCC(=O)OCCOC(=O)CCCC(=O)OCCOC(=O)CCCC(=O)OCCOC(=O)CCCC(=O)OCCO1
{[][<]C(=O)CC(C)O[<], [>]C(=O)COC(=O)CO[>][]} (*)	C1(=O)CC(C)OC(=O)CC(C)OC(=O)COC(=O)COC(=O)CC(C)OC(=O)CC(C)OC(=O)C OC(=O)COC(=O)CC(C)OC(=O)CC(C)OC(=O)COC(=O)COC(=O)CC(C)OC(=O)CC(C) OC(=O)COC(=O)COC(=O)CC(C)OC(=O)CC(C)OC(=O)COC(=O)COC(=O)CC(C)OC(=O)CC(C)OC(=O)COC(=O)COC(=O)CC(C)OC(=O)CC(C)OC(=O)COC(=O)COC(=O) CC(C)OC(=O)CC(C)OC(=O)COC(=O)CO1

Table S9: RDKit descriptors used for polyester database vectorization.

DBalabanJ	DTPSA
DBertzCT	Dfr_Ar_N
DMolLogP	Dfr_C_O
DMolMR	Dfr_C_O_noCOO
DMolWt	Dfr_NH0

DNOCount	Dfr_Ndealkylation1
DNumAliphaticCarbocycles	Dfr_aryl_methyl
DNumAliphaticHeterocycles	Dfr_benzene
DNumAliphaticRings	Dfr_bicyclic
DNumAromaticCarbocycles	Dfr_ester
DNumAromaticHeterocycles	Dfr_ether
DNumAromaticRings	Dfr_furan
DNumHAcceptors	Dfr_lactone
DNumHeteroatoms	Dfr_methoxy
DNumRotatableBonds	Dfr_para_hydroxylation
DNumSaturatedCarbocycles	Dfr_pyridine
DNumSaturatedHeterocycles	Dfr_sulfide
DNumSaturatedRings	Dfr_sulfone
DNumValenceElectrons	Dfr_unbrch_alkane

Table S10: Vector sizes for RDKit and Morgan fingerprinting.

Generated vector size	Final RDKit fingerprinting vector size	Final Morgan fingerprinting vector size
50	41	46
100	95	96
150	149	146
200	197	196
250	249	246
300	299	294
350	249	332
400	400	377
450	450	429
500	499	465
550	550	499
600	600	529

Table S11: Optimal values of classification hyperparameters.

Model	Dataset	Vector	Validation accuracy	Vector size	Number of trees	Maximum depth	Maximum leaf nodes
Random forest	All	Morgan fingerprinting	0.743	300	2^7	16	32
	All	RDKit fingerprinting	0.817	300		4	16
	All	RDKit descriptors	0.743	38		8	16
	Physical state	Morgan fingerprinting	0.657	250		8	32
	Physical state	RDKit fingerprinting	0.771	300		4	8
	Physical state	RDKit descriptors	0.729	38		4	16
	Molecular weight	Morgan fingerprinting	0.794	250		16	32
	Molecular weight	RDKit fingerprinting	0.794	250		8	8
	Molecular weight	RDKit descriptors	0.824	38		2	16
	Both	Morgan fingerprinting	0.700	100		8	16
	Both	RDKit fingerprinting	0.700	250		4	8
	Both	RDKit descriptors	0.733	38		4	8
Logistic classification	All	Morgan fingerprinting	0.780	350			
	All	RDKit fingerprinting	0.743	200			
	All	RDKit descriptors	0.716	38			
	Physical state	Morgan fingerprinting	0.600	250			
	Physical state	RDKit fingerprinting	0.686	100			
	Physical state	RDKit descriptors	0.700	38			
	Molecular weight	Morgan fingerprinting	0.794	250			
	Molecular weight	RDKit fingerprinting	0.882	100			
	Molecular weight	RDKit descriptors	0.853	38			
	Both	Morgan fingerprinting	0.800	100			
	Both	RDKit fingerprinting	0.767	200			
	Both	RDKit descriptors	0.767	38			

Table S12: Confusion matrix values for the validation split for each model, dataset and vectorization.

Dataset	Vectorization	Model	True positives	True negatives	False positives	False negatives	Total
All polymers	Morgan fp	Logistic reg.	38	47	9	15	109
		Random Forest	36	45	11	17	109
	RDKit fp	Logistic reg.	34	47	9	19	109
		Random Forest	39	50	6	14	109
	RDKit descriptors	Logistic reg.	33	45	11	20	109
		Random Forest	35	44	12	18	109
Physical State and Molecular Weight	Morgan fp	Logistic reg.	16	8	5	1	30
		Random Forest	14	7	6	3	30
	RDKit fp	Logistic reg.	15	8	5	2	30
		Random Forest	13	8	5	4	30
	RDKit descriptors	Logistic reg.	15	8	5	2	30
		Random Forest	15	9	4	2	30
Physical State	Morgan fp	Logistic reg.	21	21	12	16	70
		Random Forest	23	22	11	14	70
	RDKit fp	Logistic reg.	26	22	11	11	70
		Random Forest	31	23	10	6	70
	RDKit descriptors	Logistic reg.	25	24	9	12	70
		Random Forest	26	23	10	11	70
Molecular weight	Morgan fp	Logistic reg.	16	11	4	3	34
		Random Forest	17	10	5	2	34
	RDKit fp	Logistic reg.	18	12	3	1	34
		Random Forest	16	12	3	3	34
	RDKit descriptors	Logistic reg.	17	12	3	2	34
		Random Forest	17	11	4	2	34

VII. References

1. Lin T-S, *et al.* (2019) BigSMILES: A Structurally-Based Line Notation for Describing Macromolecules. *ACS Central Science* 5(9):1523-1531.
2. Singhvi MA-O, Zinjarde SS, & Gokhale DA-O (Polylactic acid: synthesis and biomedical applications. (1365-2672 (Electronic)).
3. De Hoe GX, *et al.* (2018) Sustainable Polyester Elastomers from Lactones: Synthesis, Properties, and Enzymatic Hydrolyzability. *J Am Chem Soc* 140(3):963-973.
4. Morgan PW (2011) Interfacial Polymerization. *Encyclopedia of Polymer Science and Technology*.
5. Nakamura H, Imanishi S, Sanui K, & Ogata N (1979) Synthesis of Aromatic Polyesters by Interfacial Polycondensation Using Immiscible Binary Solvents. *Polymer Journal* 11(8):661-664.
6. Binczak J, Dziuba K, & Chrobok A (2021) Recent Developments in Lactone Monomers and Polymer Synthesis and Application. *Materials (Basel)* 14(11).
7. Numata K, Abe H, & Iwata T (2009) Biodegradability of Poly(hydroxyalkanoate) Materials. *Materials* 2:1104 - 1126.
8. Shah AA, Hasan F, Hameed A, & Ahmed S (2008) Biological degradation of plastics: A comprehensive review. *Biotechnology Advances* 26(3):246-265.
9. Elbanna K, Lütke-Eversloh T, Jendrossek D, Luftmann H, & Steinbüchel A (2004) Studies on the biodegradability of polythioester copolymers and homopolymers by polyhydroxyalkanoate (PHA)-degrading bacteria and PHA depolymerases. *Archives of Microbiology* 182:212-225.
10. Briese BH, Schmidt B, & Jendrossek D (1994) Pseudomonas lemoignei has five poly(hydroxyalkanoic acid) (PHA) depolymerase genes: A comparative study of bacterial and eukaryotic PHA depolymerases. *Journal of Environmental Polymer Degradation* 2:75-87.
11. Knoll M, Hamm TM, Wagner F, Martinez V, & Pleiss J (2009) The PHA Depolymerase Engineering Database: A systematic analysis tool for the diverse family of polyhydroxyalkanoate (PHA) depolymerases. *BMC Bioinformatics* 10:89.
12. Augusta J, Miiller R-J, & Widdecke H (1993) A rapid evaluation plate-test for the biodegradability of plastics. *Appl Microbiol Biotechnol* 39:673-678.
13. Teeraphatpornchai T, *et al.* (2003) Isolation and characterization of a bacterium that degrades various polyester-based biodegradable plastics. *Biotechnology Letters* 25(1):23-28.
14. Av-Ron SHM (2022) High-Throughput Clear-Zone (Zenodo).
15. Arora A, *et al.* (2021) Random Forest Predictor for Diblock Copolymer Phase Behavior. *ACS Macro Letters* 10(11):1339-1345.
16. Pedregosa FV, G.; Gramfort, A.; Michel, V.; Thirion, B.; Grisel, O.; Blondel, M.; Prettenhofer, P.; Weiss, R.; Dubourg, V. (2011) Scikit-Learn: Machine Learning in Python. *J. Mach. Learn. Res.* 12:2825-2830.
17. Willett P, Barnard JM, & Downs GM (1998) Chemical Similarity Searching. *Journal of Chemical Information and Computer Sciences* 38(6):983-996.
18. Herzog K, Müller RJ, & Deckwer WD (2006) Mechanism and kinetics of the enzymatic hydrolysis of polyester nanoparticles by lipases. *Polymer Degradation and Stability* 91(10):2486-2498.